Synthesis, characterization and catalytic applications of Fe@ST-COF for the Synthesis of Polysubstituted Pyridine

Dissertation submitted to
Visvesvaraya National Institute of Technology, Nagpur
In partial fulfilment of the requirements for the award of the degree

Master of Science

In

Chemistry

by

Pranjal Singh (MS23CHM016)

under the guidance of

Dr. Umesh R. Pratap

Department of Chemistry

Visvesvaraya National Institute of Technology

Nagpur 440010 (India)

May 2025

©Visvesvaraya National Institute of Technology (VNIT) 2025

Department of Chemistry
Visvesvaraya National Institute of Technology, Nagpur

Declaration

I, Pranjal Singh hereby declare that this dissertation titled **"Synthesis, characterization and catalytic applications of Fe@ST-COF for the Synthesis of Polysubstituted Pyridine"** is carried out by me in the Department of Chemistry of Visvesvaraya National Institute of Technology, Nagpur. The work is original and has not been submitted earlier whole or in part for the award of any degree/diploma at this or any other Institution / University.

Pranjal Singh (MS23CHM0016)
Date:

Certificate

This is to certify that the dissertation titled **"Synthesis, characterization and catalytic applications of Fe@ST-COF for the Synthesis of Polysubstituted Pyridine"** is submitted by **Pranjal Singh** in partial fulfilment of the requirements for the award of the degree of **Master of Science in Chemistry, VNIT Nagpur.** The work is comprehensive, complete and fit for final evaluation.

Dr. Umesh R. Pratap
Associate Professor
Department of Chemistry, VNIT Nagpur

Head, Department of Chemistry
VNIT, Nagpur
Date:

Visvesvaraya National Institute of Technology, Nagpur

Department of Chemistry

Non-Plagiarism Certificate

Certified that M.Sc. dissertation titled **"Synthesis, characterization and catalytic applications of Fe@ST-COF for the Synthesis of Polysubstituted Pyridine"** submitted by **Pranjal Singh** Enrollment No. **MS23CHM016** ID No. 30677 has been checked for plagiarism using TURNITIN software, and the overlap is found within prescribed limits. A summary of the report is given below.

ORIGINALITY REPORT

16%	11%	12%	%
SIMILARITY INDEX	INTERNET SOURCES	PUBLICATIONS	STUDENT PAPERS

Dr. Umesh R. Pratap
Associate Professor
Department of Chemistry
Visvesvaraya National Institute of Technology, Nagpur(440010)

Pranjal Singh
Enrollment No:MS23CHM016

Acknowledgment

I would like to express my sincere gratitude to my supervisor, **Dr. Umesh R. Pratap**, for his exceptional guidance, unwavering support, and invaluable mentorship throughout my journey as a M.Sc. student. I am forever indebted for his remarkable expertise, patience, and dedication in guiding me through conducting research and writing this thesis. Your astute insights, constructive feedback, and visionary guidance have been instrumental in shaping the direction of my work. You have consistently challenged me to think critically, encouraged me to explore new avenues of inquiry, and inspired me to reach for excellence.

I would also like to express my gratitude to my Ph.D. scholars, Ms. Shivani Bhagat, Mr. Ankit Verma, Ms. Sneha Wahurwagh and Mr. Pankaj Kumar Gautam, who have accompanied me on this academic journey. Your camaraderie, intellectual discussions, and collaborative efforts have enriched my experience in countless ways. Through our shared challenges and triumphs, I have not only grown as a researcher but also formed lasting friendships and a supportive network. Your diverse perspectives, stimulating debates, and willingness to lend a helping hand have been invaluable, and I am grateful for the opportunity to be part of such an inspiring community.

Furthermore, I would like to express my heartfelt gratitude to my lab mate, Mr. Naresh Bahalia, and all those who generously offered their help and support throughout this journey. A special note of thanks goes to my beloved Mom and Dad, whose unwavering love, encouragement, and inspiration have been the cornerstone of my strength and perseverance.

Pranjal Singh

Abstract:

Covalent Organic Frameworks (COFs) are crystalline, porous polymers built from organic building blocks connected by strong covalent bonds. They are known for their high surface area, thermal and chemical stability, and structural tunability, making them suitable for various applications, including catalysis. In this study, a porphyrin-based COF (ST-COF) was synthesized by the condensation of SL-1 (4,4'-(ethyne-1,2-diyl)dibenzaldehyde) and TAPP (meso-tetrakis(4-aminophenyl)porphyrin) under solvothermal conditions. To improve its catalytic functionality, iron ions were introduced into the porphyrin cavities of ST-COF, resulting in Fe@ST-COF. The framework was characterized by FT-IR, FESEM, EDX, TGA, BET, and ICP analysis. These results confirmed the successful formation of the COF structure and the effective incorporation of iron into the framework. SEM analysis showed that Fe@ST-COF exhibits a uniform, sphere-like morphology. Fe@ST-COF was then used as a heterogeneous catalyst in a one-pot, multicomponent reaction to synthesize polysubstituted pyridines. The reaction proceeded efficiently with a broad range of readily available substrates, delivering good yields. This work highlights the potential of metallated COFs like Fe@ST-COF for use in sustainable and practical catalytic transformations, combining the benefits of COF porosity, stability, and metal coordination sites.

S.No.	Title of Figures	Page no.
1	Illustration showing synthetic routes, properties and applications of COFs	3
2	Schematic representation of building blocks combined with different geometry to synthesize COFs	4
3	Self-condensation reaction and Co-Condensation Reaction.	5
4	Condensation reactions of imine COFs	7
5	Synthesis of PI COF	8
6	Triazine based COF	9
7	Schematic diagram showing solvothermal synthesis of COFs	10
8	Reaction showing synthesis of COF by Microwave method	11
9	Condensation reaction of 2,6-dicyanonaphthalene forming a distinct trimer and then a CTF by ionothermal method	13
10	Reaction showing synthesis of COF by Mechanochemical process	13
11	COF as a catalyst for coupling reactions	17
12	Suzuki-Miyaura reaction by Pd/COF.	17
13	TAPP-TT-COF synthesis by encapsulating functionalised Ag(NPs)	18
14	Schematic formation of COF-609 for CO_2 capture	20
15	FT-IR analysis of TAPP	31
16	FTIR of SL-1,TAPP,ST-COF and Fe@ST-COF	32
17	PXRD of TAPP, SL 1,ST-COF and Fe@ST-COF	33
18	TGA analysis of ST-COF and Fe@ST-COF	34
19	Nitrogen sorption isotherm of ST-COF	35
20	(a) Fe2p spectra and (b) Full elemental survey spectra of Fe@ST-COF	36
21	FE-SEM Images of ST-COF	37
22	FE-SEM Images of Fe@ST-COF	38
23	ST-COF (a) Elemental mapping and (b) SEM-EDS analysis	40
24	Fe@ST-COF (a) Elemental mapping and (b) SEM-EDS analysis	41

25	Picture of some natural polysubstituted pyridine	44
26	Picture of some synthetic polysubstituted pyridine	44
27	Synthesis of DHPM via Biginelli Reaction	45
28	Plausible reaction mechanism route	47

LIST OF CONTENTS

CHAPTER-1	Page No.
1 Introduction	1
1.1 Covalent Organic Frameworks	2
1.2 Coupling Chemistry and topologies	3
1.3 Classifications	4
1.3.1 Boron-containing's COFs	5
1.3.2 Imine-linked COFs	6
1.3.3 Imide-linked COFs	7
1.3.4 Triazine-based COFs	8
1.4 Method of Synthesis	9
1.4.1 Solvothermal approach	10
1.4.2 Microwave Synthesis	11
1.4.3 Ionothermal Synthesis	12
1.4.4 Mechanochemical Synthesis	13
1.5 Application of COFs	14
1.5.1 Catalysis	15
1.5.1.1 Metal containing CCOFs as a Catalyst	15
1.5.1.2 COF in a meatal free catalysis	19
1.5.2 Photocatalytic and Electronic application of COFs	20
1.5.3 COFs in Drug delivery systems	21
CHAPTER-2	24
2 Synthesis and characterizations of Fe loaded TAPP-ST based COF	25
2.1 Introduction of TAPP based COF	25
2.2 Experimental Sections	27
2.2.1 Material required for synthesis of TAPP	27
2.2.2 Material required for synthesis of SL-1	28

2.2.3 Material required for synthesis of ST-COF 29
2.2.4 Synthesis of Iron(III) loaded COF as a Fe@ST-COF 30
2.3 Characterization of SL-1, TAPP, ST-COF, Fe@ST-COF 31
2.3.1 FT-IR study of TAPP 31
2.3.2 Comparative FT-IR 32
2.3.3 XRD analysis 33
2.3.4 BET analysis 34
2.3.5 TGA analysis of ST-COF and Fe@ST-COF 35
2.3.6 XPS analysis of Fe@ST-COF 36
2.3.7 FESEM results of ST-COF 37
2.3.8 FESEM results of Fe@ST-COF 38
2.3.9 EDS analysis and Elemental Mapping 39

CHAPTER-3 42

3 Catalytic application of Fe@ST-COF as a heterogeneous catalyst for synthesis of poly-substituted pyridine 43
3.1 Introduction to MCRs for synthesis of pyridine and their uses 43
3.2 Results and discussion 46
3.3 Plausible mechanism 47
3.4 Experimental Section 48
3.4.1 Material required 48
3.4.2 General procedure 48
3.4.3 Observation Table 49
3.5 NMR Spectral Data 52
3.6 Conclusion 54

CHAPTER-1

INTRODUCTION

1.1 Covalent Organic Frameworks:

Covalent organic frameworks (COFs) have emerged as an up-and-coming class of crystalline organic porous materials. This is due to their exceptional structural tunability and organic building blocks' atomically precise spatial organization. These frameworks are constructed via reversible covalent bond formation between carefully selected molecular linkers, leading to extended two or three-dimensional networks. [1] [2] [3] [4] [5] The geometry and the topology of the resulting COFs are predetermined by the size, symmetry, connectivity, and constituent linkers. Unlike conventional linear polymers, COFs offer a unique advantage in enabling positional control over their building blocks, thereby allowing for the deliberate design of a structurally ordered framework with tailored chemical and physical properties.

The intrinsic porosity and regularity of COFs result in well-defined nanochannels and cavities, which provide an ideal environment for various applications, including molecular storage, controlled release, and selective separation. Furthermore, the large and chemically tunable internal surface area of COFs makes them particularly attractive for catalytic and sensing applications. Due to the pi-conjugation and ordered arrangement of the building units, COFs also hold significant potential in electronic and optoelectronic applications, such as charge transport, photovoltaics, and electrochemical energy storage systems.

Positioned at the intersection of metal-organic frameworks (MOFs) and amorphous porous organic polymers, such as porous aromatic frameworks and polymers with intrinsic microscopy, COFs distinguished themselves through their crystallinity and modularity. Since their initial discovery in 2005, the field has expanded rapidly, with a broad spectrum of structures and compositions realized, highlighting the immense design space that COFs offer.

This thesis aims to provide a comprehensive overview of the foundational principle underlying COF synthesis and design. [6] [7] [8] [9] [10] The discussion will begin with an examination of the key prerequisites for COF formation, including the reversible coupling reactions commonly employed. A systematic summary of the structural motifs reported to date will be represented through a series of classification matrices. In addition to the primary assembly of frameworks, strategies for introducing additional functionalities via post-synthetic modification will be explored, demonstrating the

versatility of COFs in accommodating diverse functional groups. Furthermore, various synthetic approaches and the influence of reaction conditions on the morphology and crystallinity versus amorphous structures. [11] Finally, the thesis will discuss the wide range of properties and practical applications of COFs across multiple fields, thereby illustrating their potential for further development and deployment in advanced material systems.

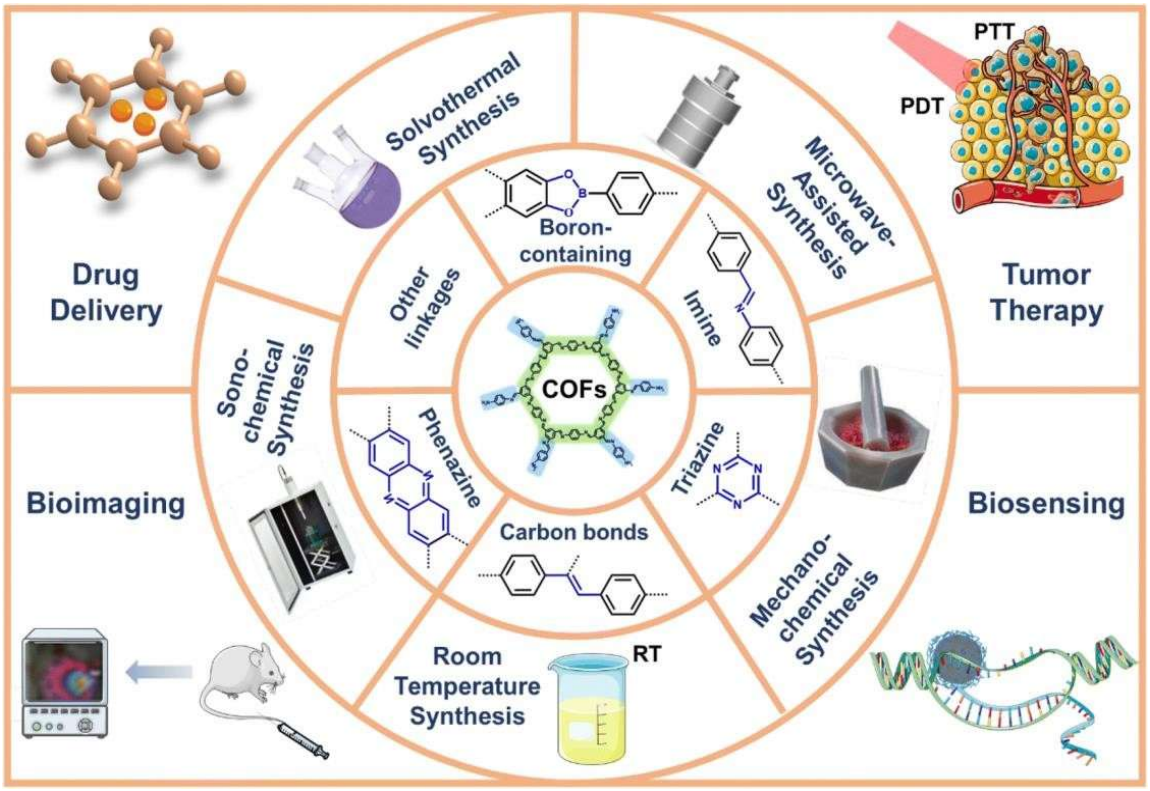

Fig.1: Illustration showing synthetic routes, properties and applications of COFs [12]

1.2 Coupling Chemistry and topologies:

Covalent organic frameworks are constructed from organic linkers through mildly reversible condensation reactions. The covalent bonds form within this framework, providing them with high thermal stability. At the same time, the reversible nature of the bonding allows for structural rearrangement and error correction during formation, which leads to crystalline, rather than amorphous, architectures. The earliest COFs were synthesized through the self-condensation of boronic acids and catechol's, resulting in five-membered boronic ester rings, or through the self-condensation of boronic esters into

boroxines. Since then, numerous other chemical reactions have been utilized for COF synthesis as shown in Figure 1 and listed in the table, which includes less commonly used pathways. Because boroxines and boronic esters are prone to hydrolysis, researchers aimed to develop more hydrolytically stable linkages. This was achieved with the introduction of imine bonds formed by condensing aldehydes and primary amines. These structures exhibit high resistance to both acidic and basic environments. The shape and connectivity of the linkers define the geometry of the COF lattice. For example, trigonal planar units can form hexagonal pores in sheet-like structures, while combining tetragonal and linear linkers produces tetragonal pores. These sheets can stack into layers, resulting in a framework with one-dimensional channels. COFs composed of such stacked 2D layers are known as 2D COFs, whereas 2D COFs consist of units with 3D connectivity, forming a fully 3D network.

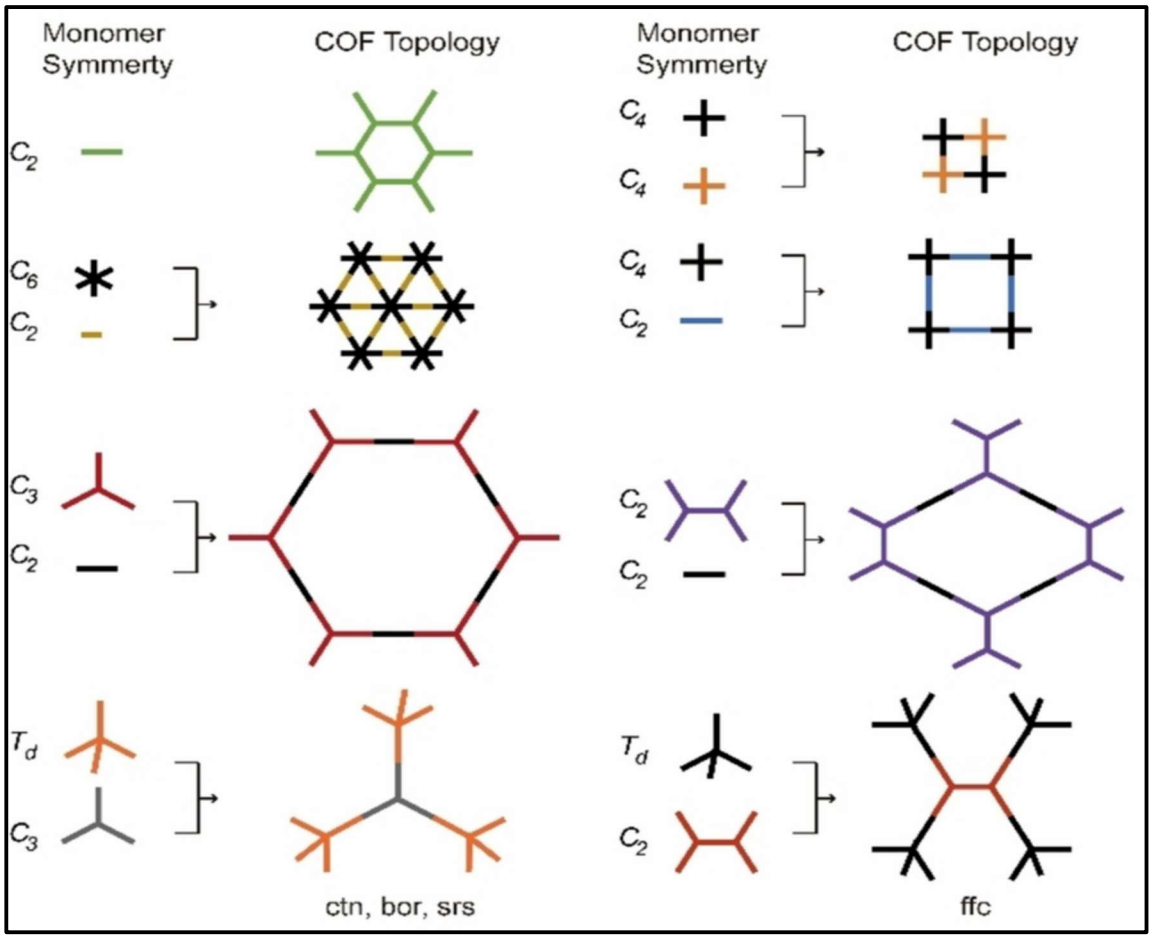

Fig.2: Schematic representation of building blocks combined with different geometry to synthesize COFs. [13]

1.3 Classification:

1.3.1 Boron-containing COFs:

Self-condensation of a single building unit:

One common method for synthesizing boron-based COFs involves the self-condensation of identical molecular units. [14] For instance, COF-1 can be synthesized using the self-condensation of 1,4-benzene boronic acid (BDBA). In this, the boronic acid groups react to form boronate anhydrides, specifically producing planar six-membered B3O3 rings known as boroxines.

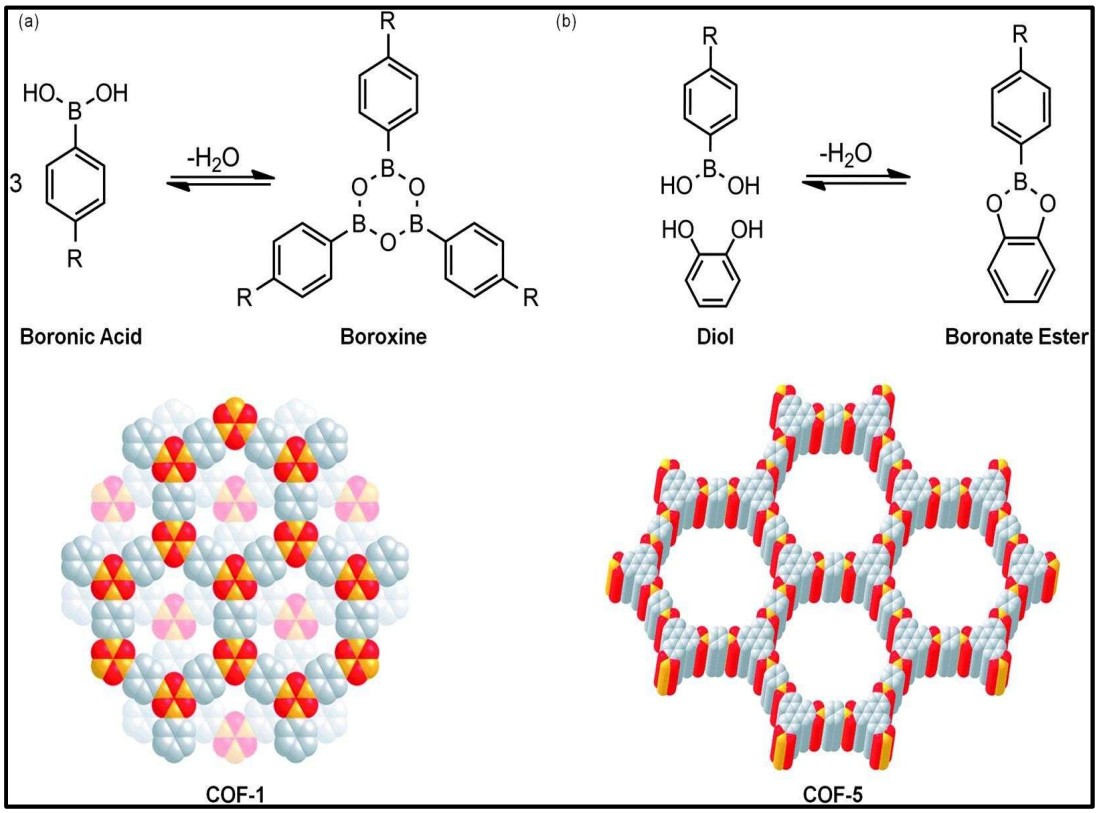

Fig.3: Self-condensation reaction and Co-Condensation Reaction.

Co-condensation of multiple building units:

An alternative approach to developing boron-based COFs involves co-condensing two or more distinct molecular units. [15] This method combines different building blocks,

enabling the integration of various functional groups. As a result, it supports the creation of 3D COFs with larger surface areas than 2D equivalents.

1.3.2 Imine-linked COFs:

Imine-based covalent organic frameworks are built upon the reversible formation of imine bonds and were first developed by Yaghi and his team in 2009 with the creation of COF-300. [16] These COFs are mainly classified into two categories, based on how the carbon-nitrogen (C=N) bond is formed.

Schiff base COFs:

This type arises from the co-condensation of aldehydes and amines. The process begins with condensation between the aldehyde and the amine group to form the Schiff base, which then undergoes polymerization to produce the framework.

Hydrazone COFs:

The second type involves the co-condensation of aldehyde with hydrazides. In this case, the aldehyde reacts with hydrazides to produce a hydrazone linkage, followed by polymerization to complete the COFs. [17]

Both Schiff-base and hydrazone-based imine COFs are known for properties like high porosity, adjustable structural features, and stability to incorporate various functional groups. These characteristics are achieved by carefully choosing the appropriate building units, which allows for a wide range of potential applications.

Chemical stability:

Imine-based COFs generally show good stability in neutral and acidic environments. However, they might be less stable under basic conditions due to possible hydrolysis of the imine linkage.

Thermal stability:

These COFs usually exhibit strong resistance to high temperatures, making them appropriate for use in elevated thermal conditions.

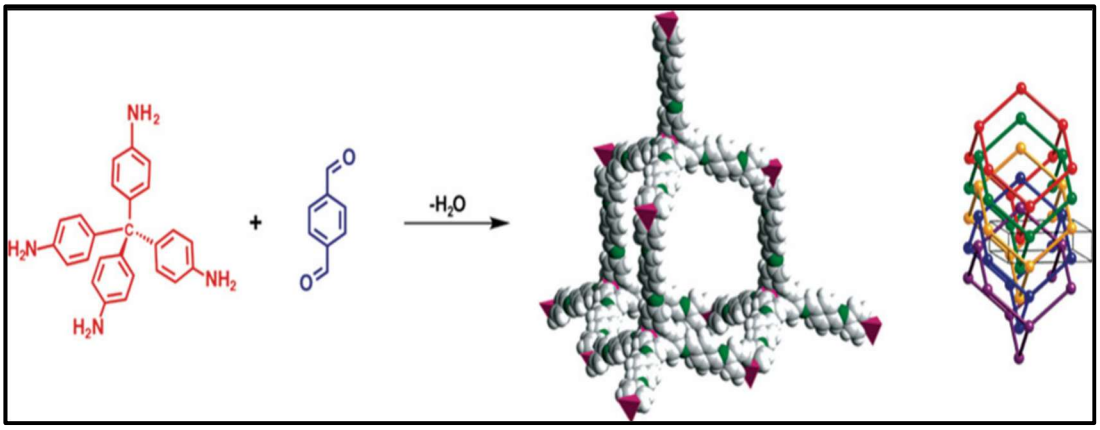

Fig 4: Condensation reactions of imine COFs. [18]

1.3.3 Imide-linked COFs:

Imide-linked COFs belong to the category of crystalline porous materials that feature imide (-C=O-N-) linkages in their structural framework. These COFs are generally produced through a condensation reaction involving amines and aldehyde or diketone-based precursors. This is followed by a thermal cyclization process that forms the imide bonds. These linkages contribute significantly to the structural integrity and crystalline order of the COF, offering excellent thermal and chemical stability.

Imide-linked COFs possess various tunable characteristics such as adjustable pore sizes, surface areas, and functional chemistry, which make them suitable candidates for application in gas storage, separation, catalysis, and sensing. In our synthesis, imide-linked COFs were prepared using dianhydride and melamine, dissolved in DMF, through a solvothermal method carried out at 140 °C over three days.

THERMAL STABILITY:

Imide bonds provide excellent thermal endurance, making imide-linked COFs ideal for environment that demands resistance to high temperatures.

CHEMICAL RESISTANCE:

The presence of the imide functional group enhances the chemical robustness of the framework, allowing it to perform effectively even in harsh chemical conditions.

MECHANICAL PROPERTIES:

Due to the structural rigidity offered by the imide group, the COFs demonstrate superior mechanical strength and durability.

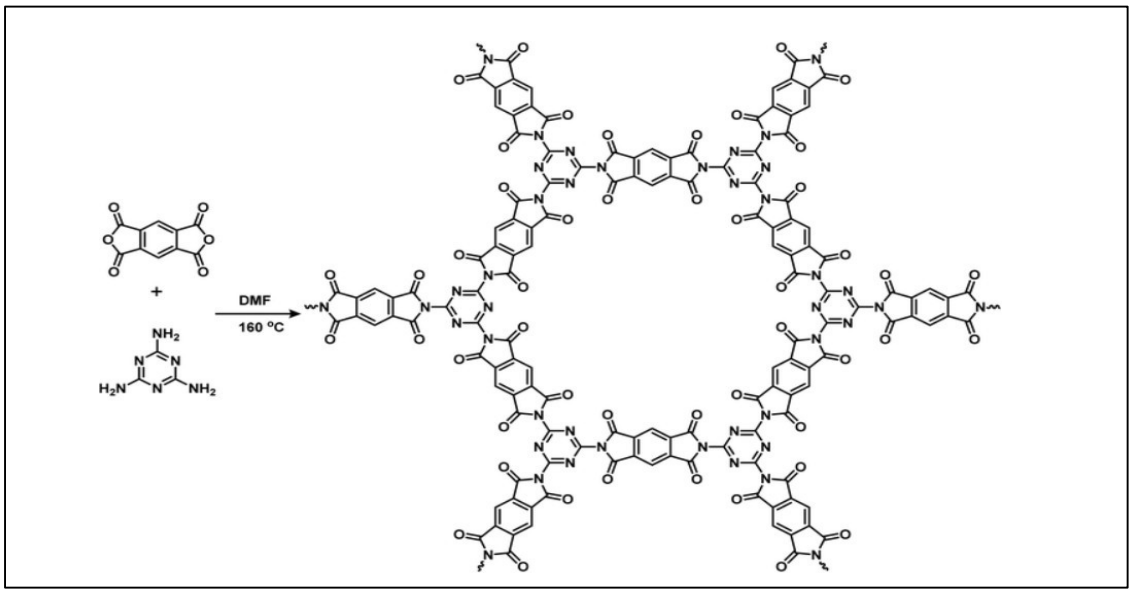

Fig.5: Synthesis of PI COF. [19]

1.3.4 Triazine-based COFs (CTFs):

Triazine-based COFs, commonly referred to as CTFs (Covalent Triazine Framework), have attracted attention due to their promising applications in gas storage, catalysis, and optoelectronics. Their appeal lies in their large surface area, excellent thermal resistance, and chemical durability. These COFs are synthesized through the polymerization of triazine rings using a variety of synthetic approaches.

To fabricate a covalent triazine framework, nitrile-containing monomers undergo cyclotrimerization, typically in the presence of zinc chloride at elevated temperatures (around 400oc). For instance, one common method involves the cyclotrimerization of 1,4-dicyanobenzene to form the desired framework.

What sets triazine-based COFs apart is their high crystallinity and consistent structural arrangement. These features distinguish them from other COF types, such as boron or imine-linked frameworks. The unique characteristics of CFTs make them ideal for cutting-edge materials research.

HIGH SURFACE AREA:

CTFs are known for having a large internal surface area, which makes them highly effective for applications in gas capture and storage. This property is particularly advantageous for hydrogen storage, carbon capture, and gas separation processes.

THERMAL STABILITY:

Due to the robust triazine bonds, CFTs are capable of retaining their structural framework even under extreme heat, making them ideal candidates for high-temperature applications.

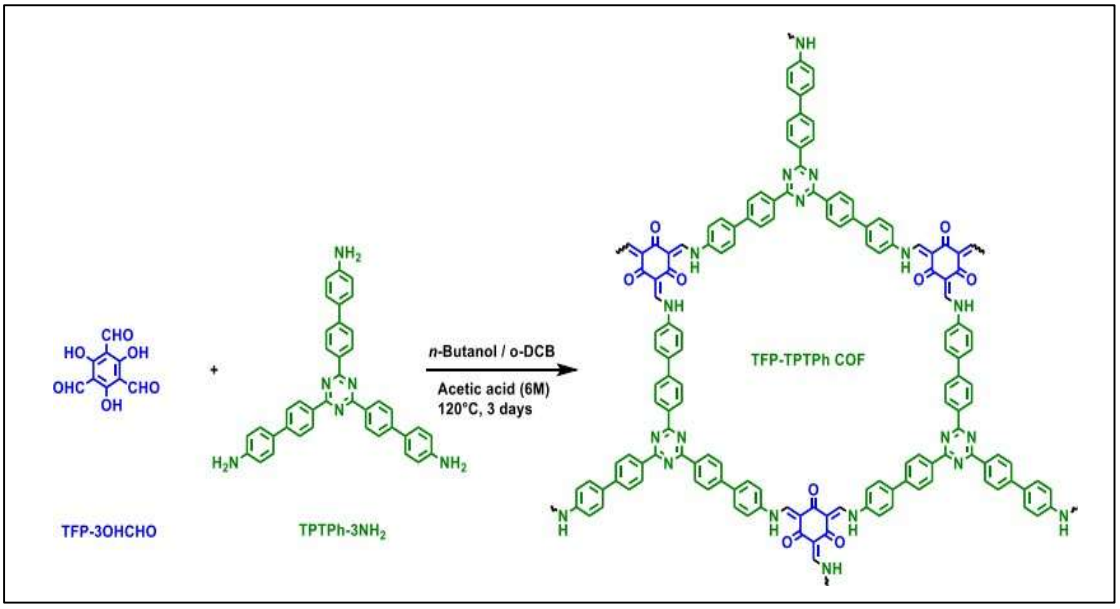

Fig 6: Triazine based COF. [20]

1.4 Method of synthesis:

When creating covalent organic frameworks, a variety of monomers, synthetic approaches, and reaction parameters-including temperature, pressure, time, and catalyst selection, are carefully considered. By optimizing these conditions, COFs with high crystallinity, porosity, and chemical stability can be obtained. The method of synthesis plays a key role in determining reaction kinetics and overall yield. Generally, COFs are synthesized using one of four main techniques: solvothermal, microwave-assisted, ionothermal, or ambient-temperature methods.

1.4.1 Solvothermal approach:

Solvothermal synthesis is the most widely used method for fabricating COFs. In this process, the reaction environment is closely controlled, especially regarding the solubility and reactivity of the starting materials, as well as the reversibility of the reactions involved. Key parameters in this method include reaction duration, temperature, the nature of the solvent, and catalyst concentration.

Typically, Pyrex or thick-walled pressure tubes with PTFE lining are employed due to their ability to maintain a sealed environment. This minimizes exposure to air and helps retain water molecules necessary for reversible bonding. The synthesis involves accurately measuring and adding monomers and solvents into the reaction vessel, followed by freeze-pump-thaw cycles to eliminate dissolved gases. The sealed tube is then heated in an oven at a controlled temperature for several days, often ranging from three to seven days.

Once the reaction concludes, the resulting product is filtered, and organic solvents are used to remove any unreacted starting materials the final COF product is collected after drying. One of the key challenges of this method is the limitation in scale, as Pyrex rubes restrict the volume of the reaction mixture. Moreover, the temperature and solvent used-such as mesitylene, 1,4-dioxane, dichlorobenzene, and n-butanol, significantly affect the quality and the crystallinity of the final COF material.

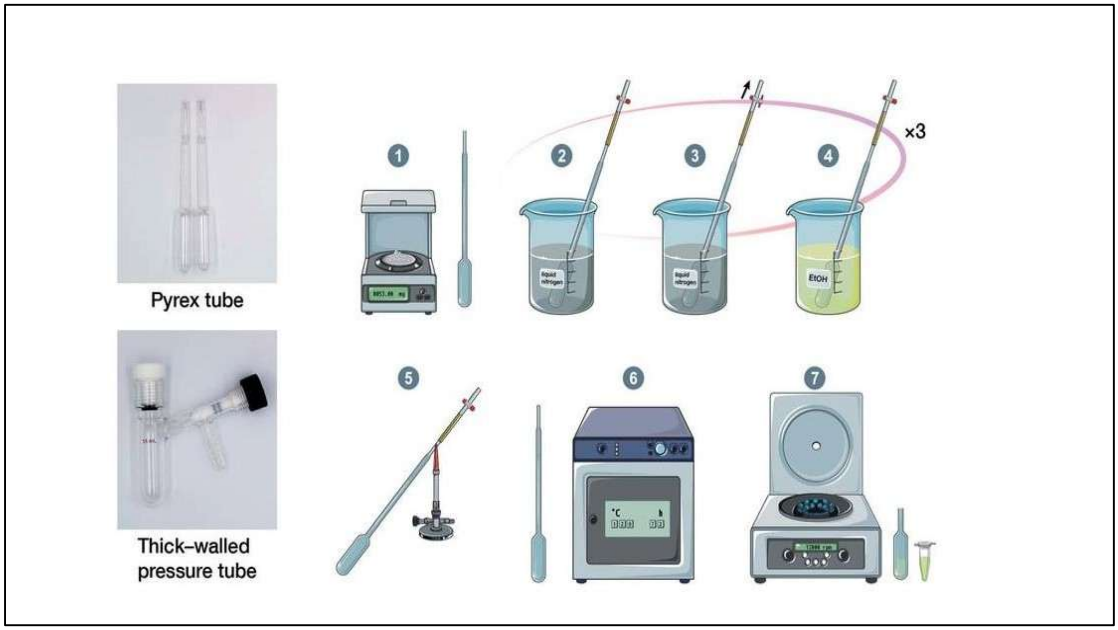

Fig 7: Schematic diagram showing solvothermal synthesis of COFs. [21]

1.4.2 Microwave synthesis:

Microwave-assisted synthesis utilizes microwave radiation to generate heat within materials themselves, distinguishing it from conventional external heating techniques that rely on conduction. This internal heating mechanism eliminates the need for external thermal transfer, allowing for rapid and uniform temperature distribution throughout the sample. Compared to traditional oven-based heating, microwave methods provide several benefits, including significantly faster reaction rates, improved yields, gentler reaction environments, reduced energy consumption, and more accurate control over reaction pathways. Cooper and his research group introduced a microwave-based technique for synthesizing Covalent Organic Frameworks (COFs).

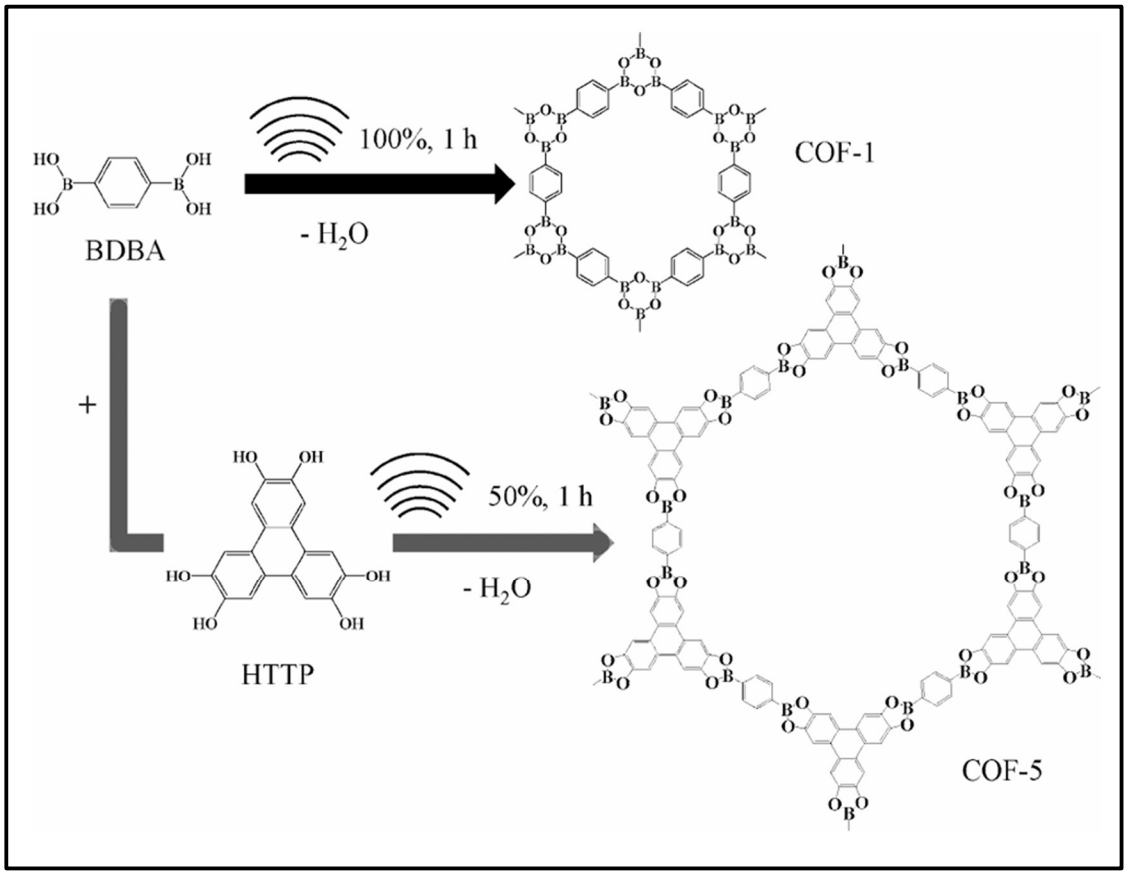

Fig 8: Reaction showing synthesis of COF by Microwave method**.** [22]

In 2009, Cooper and his team were the first to implement microwave irradiation for the synthesis of B-O-linked COF-5, achieving an impressive yield of 68%. This innovative method drastically reduced the synthesis time to approximately 20 minutes—over 200

times faster than the conventional solvothermal process, which typically requires three days. Furthermore, the COF-5 obtained through microwave heating exhibited a higher Brunauer–Emmett–Teller (BET) surface area of 2019 m^2/g, outperforming the 1590 m^2/g surface area recorded for samples produced.

1.4.3 Ionothermal Synthesis:

Ionic liquids (ILs) are organic salts that stay in a liquid state at or near ambient temperature. They are commonly regarded as eco-friendly solvents and serve as reusable substitutes for conventional volatile organic compounds. When synthesis is carried out using ILs, the process is referred to as ionothermal synthesis. This technique holds promise for industrial-scale applications, largely because it eliminates the risks associated with high-pressure systems.

Functioning both as solvents and potential structure-directing agents, ionic liquids are employed in ionothermal synthesis to generate single crystalline materials. In 2007, Thomas and his collaborators utilized this strategy to synthesize the first Covalent Organic Framework (COF).

Using these conditions, two crystalline porous compounds, CTF-1 and CTF-2, were successfully synthesized. Typically, this process involves combining the organic precursor and $ZnCl_2$ in a Pyrex ampule, which is then evacuated, hermetically sealed, and subjected to heat treatment at 400 °C for 40 hours. Once cooled to ambient temperature, the reaction mixture is crushed and rinsed thoroughly with water to remove excess $ZnCl_2$. The obtained powder is then stirred in a diluted hydrochloric acid solution for about 15 hours to ensure further removal of $ZnCl_2$, followed by filtration, successive washes with water and tetrahydrofuran (THF), and final drying under reduced pressure to yield CTF-1 and CTF-2.Besides serving as a reactive medium that drives the cyclotrimerization of aromatic nitrile monomers like 2,6-dicyanonaphthalene, molten $ZnCl_2$ also behaves as an ionic liquid at elevated temperatures (400 °C). This environment enables the formation of Covalent Triazine Frameworks (CTFs) with high degrees of crystallinity and thermal resilience. Nevertheless, the limited availability of suitable monomers poses a significant limitation, given the harsh reaction parameters required for this method.

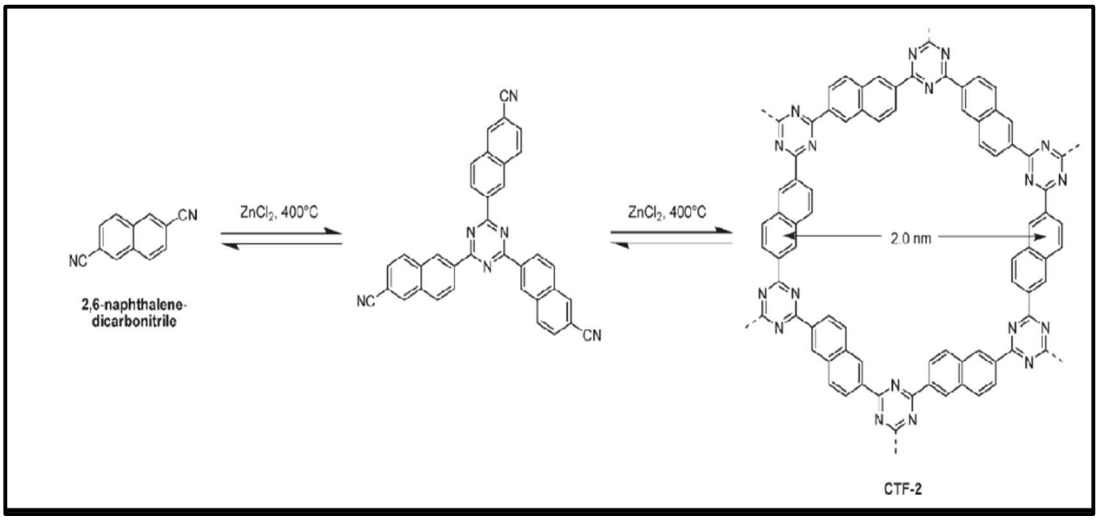

Fig 9: Condensation reaction of 2,6-dicyanonaphthalene forming a distinct trimer and then a CTF by ionothermal method**.** [23]

1.4.4 Mechanochemical Synthesis:

In the image, the process begins by mixing 1,3,5-triformylphloroglucinol (Tp) with diamine compounds (Pa-R) to initiate a Schiff base condensation reaction.

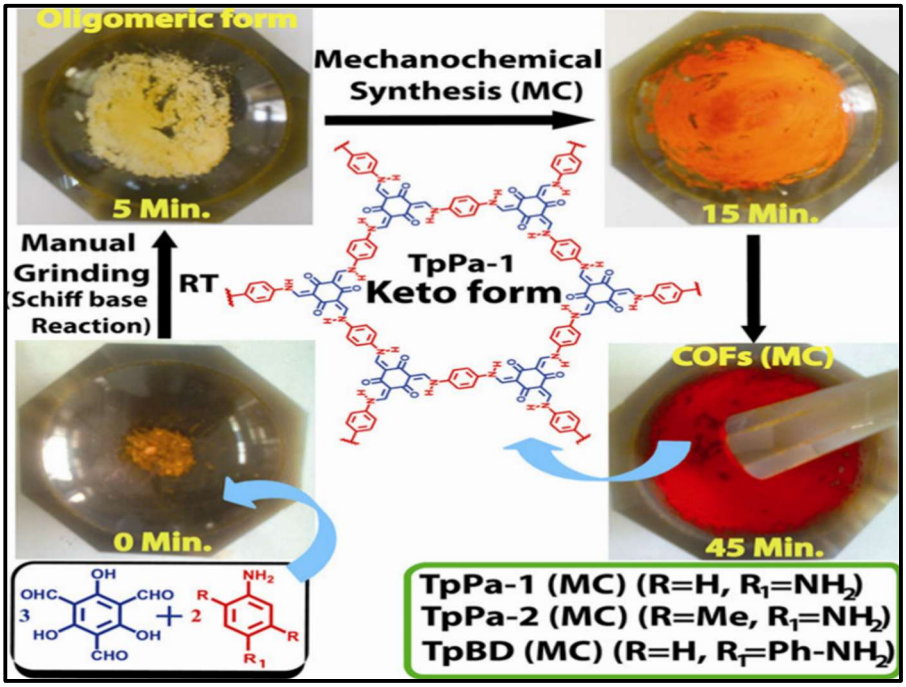

Fig 10: Reaction showing synthesis of COF by Mechanochemical process**.** [24]

At 0 minutes, the starting materials are visibly mixed. After 5 minutes of manual grinding, the reaction advances to form an oligomeric intermediate. Continuing the mechanochemical process for 15 minutes leads to a more developed intermediate stage. Eventually, after 45 minutes, the reaction yields a bright red solid corresponding to the crystalline COF (TpPa-1) in its keto form, confirmed by the color transformation. This method avoids the use of solvents and high temperatures, making it more environmentally sustainable. Moreover, it provides rapid synthesis of highly crystalline COFs such as TpPa-1, TpPa-2, and TpBD, depending on the specific diamine (R, R_1 groups) used in the reaction.

1.5 APPLICATION OF COF:

Covalent Organic Frameworks (COFs) are exceptionally adaptable materials that demonstrate great potential across a broad spectrum of practical and industrial applications. Their distinct physicochemical characteristics make them dependable candidates for numerous advanced technologies. Characterized by their large surface areas, well-ordered porous architectures, and tunable functionalities, COFs serve as excellent platforms for tasks such as gas storage and separation, heterogeneous catalysis, and electronic or optoelectronic applications. Similar to other porous materials like zeolites, zeolitic imidazolate frameworks (ZIFs), metal-organic frameworks (MOFs), and porous carbon-based materials, COFs offer significant advantages in terms of efficiency and structural versatility.

What sets COFs apart is their remarkable thermal and chemical resilience. Unlike many hybrids organic-inorganic systems, COFs are composed of light, earth-abundant elements such as carbon, boron, hydrogen, oxygen, and nitrogen, which are interconnected through robust covalent bonds. This intrinsic bonding network contributes to their enhanced durability and stability under harsh environmental conditions, making them ideal for long-term usage in demanding applications like energy storage, environmental remediation, and sustainable chemical synthesis. Moreover, their modular design enables precise control over pore size, shape, and functionalization, further expanding their usefulness across emerging technological fields.

1.5.1 Catalysis:

Covalent Organic Frameworks (COFs) commonly exhibit a highly ordered, mesh-like structure with uniformly distributed nanopores that allow the passage and accommodation of external molecules measuring just a few nanometers in size. This structural feature significantly enhances their potential in catalytic processes. The biologically inspired layout of COFs also enables straightforward customization of their functional groups.

The integration of compatible chemical functionalities into the COF framework can result in remarkable optical and optoelectronic behaviors. A wide selection of monomeric units with varying configurations and levels of porosity can be employed to construct COFs with desired characteristics. Thanks to their large surface area, exceptional structural robustness, interconnected pore systems, and adaptability, COFs are regarded as outstanding catalytic materials.

Their impressive resilience to heat and chemicals makes COFs reliable under rigorous reaction environments. The consistent and symmetrical arrangement of pores further supports effective molecular diffusion and enhances both catalytic efficiency and product selectivity. Altogether, COFs emerge as highly promising materials for driving diverse chemical reactions—such as organic synthesis, reduction (hydrogenation), and oxidative processes—delivering a greener and more effective route for catalysis in modern chemistry.

1.5.1.1 Metal containing COFs as a catalyst:

i) C–C Coupling Reactions:

Carbon–carbon bond-forming reactions represent a cornerstone of contemporary organic synthesis. Around 85% of developments in the synthesis of fine chemicals, pharmaceuticals, agrochemicals, and household products rely on catalytic C–C coupling strategies. These transformations are traditionally carried out using homogeneous transition metal complexes, especially palladium-based systems like the renowned Suzuki–Miyaura and Heck cross-coupling protocols. However, the application of Covalent Organic Frameworks (COFs) as catalysts in such reactions has gained attention due to several compelling benefits:

Lower Environmental Footprint:

Homogeneous Pd catalysts present notable challenges, especially in pharmaceutical applications, due to the toxicity of residual noble metals. Moreover, the recovery and purification of these metal catalysts are often inefficient and costly, contributing significantly to the overall expenses of drug manufacturing. COFs, by contrast, offer a cleaner and more sustainable alternative.

Improved Catalytic Performance:

Incorporating metal centers within the COF matrix confines them in a fixed position, which can initially appear to hinder the movement of substrates and release of products. However, this spatial restriction actually aids in preserving the catalytic site's activity. Unlike MOFs, which feature metal nodes that may interfere with catalytic behavior, COFs do not contain extraneous transition metals, reducing the risk of side reactions and enhancing catalytic precision.

In essence, COFs provide a greener, more efficient platform for catalyzing C–C coupling reactions, addressing many of the drawbacks associated with conventional Pd-based homogeneous systems.

A significant development in this area was reported by Wang and coworkers in 2011, when they introduced COF-LZU1, a two-dimensional imine-linked framework with promising catalytic properties. It was synthesized via a straightforward condensation reaction between 1,3,5-triformylbenzene and 1,4-diaminobenzene, resulting in a well-ordered, layered structure that simplified its construction.

Subsequently, a mild, room-temperature post-synthetic modification enabled the introduction of palladium into the COF network. By treating the framework with palladium acetate ($Pd(OAc)_2$), the team successfully produced a Pd/COF-LZU1 composite with uniformly distributed catalytic centers.

This hybrid catalyst demonstrated excellent activity in the Suzuki–Miyaura cross-coupling reaction, a widely employed method for forging C–C bonds. Pd/COF-LZU1 efficiently promoted the coupling of aryl halides with arylboronic acids, yielding the desired products with high effectiveness, thus confirming its utility in practical organic synthesis.

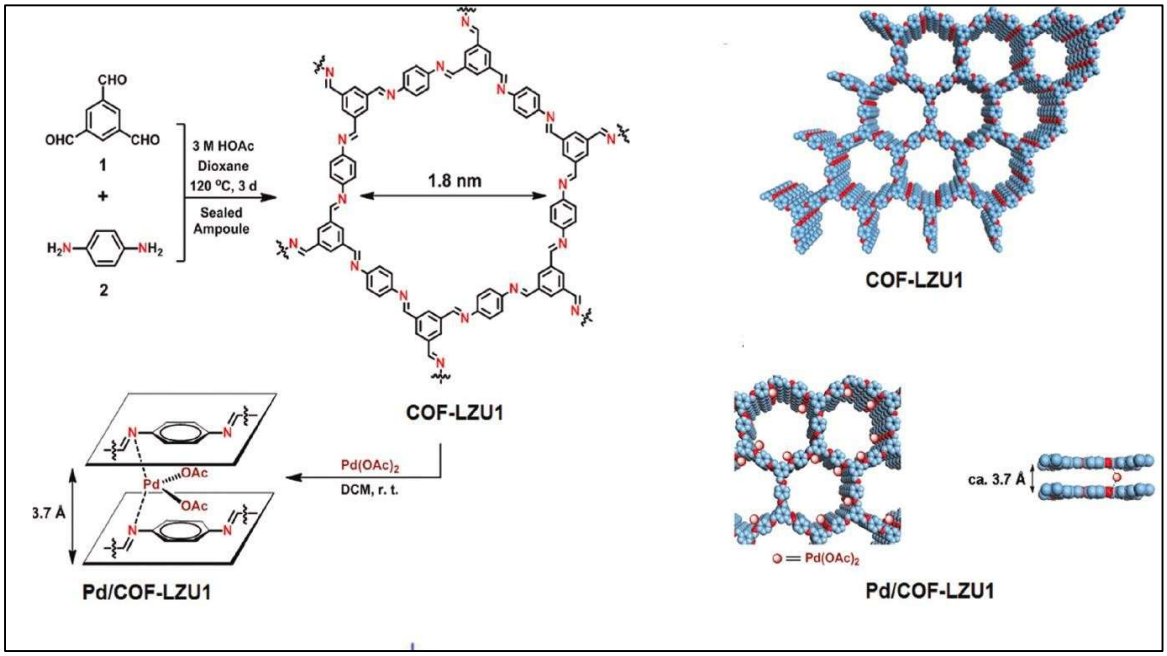

Fig.11: COF as a catalyst for coupling reactions**.** [25]

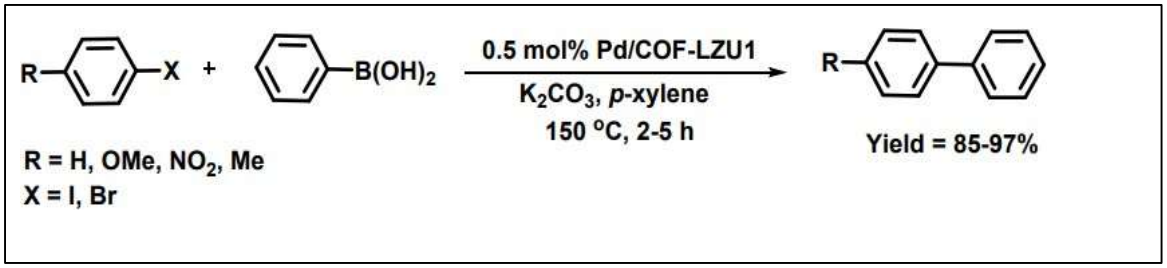

Fig. 12: Suzuki-Miyaura reaction by Pd/COF.

ii) Oxidation reactions:

Thomas and his research team recently utilized a porous crystalline framework (PCF) as a support material for palladium (Pd) nanoparticles in the catalytic oxidation of glycerol in a solvent medium. These PCFs, characterized by their high nitrogen content, serve as effective hosts for stabilizing metal nanoparticles, preventing issues such as agglomeration or catalyst leaching. The Pd nanoparticles immobilized on the PCF exhibited an average diameter of approximately 3.08 nanometers. The resulting catalyst, designated as Pd@PCF, demonstrated outstanding catalytic efficiency by achieving full conversion of glycerol into glycerate within a span of three hours. [26] [27] [28]

The superior catalytic behavior of Pd@PCF can be attributed to the synergistic interaction between the palladium particles and the nitrogen-rich PCF framework. The PCF provides

a highly stable and uniformly distributed matrix that enhances the dispersion and stability of the Pd nanoparticles, thereby promoting high activity and selectivity during the oxidation process. This research highlights the promise of PCF-supported catalysts in delivering efficient, sustainable, and eco-conscious solutions for chemical transformations.

iii) Reduction reactions:

A series of Ag@TAPP-COF hybrid materials were effectively fabricated, featuring high surface areas and well-organized porous architectures. The extended π-conjugated system of the TAPP-COF framework was enriched with multiple nitrogen and sulphur coordination sites, which played a key role in enhancing reagent adsorption and facilitating the immobilization of Ag^{+} ions. Owing to these structural merits, the Ag@TAPP-COF composites were employed as heterogeneous catalysts for the reduction of 4-nitrophenol (4-NP). Among the tested variants, Ag10@TAPP-COF demonstrated superior catalytic efficiency, displaying excellent durability and recyclability.

Further analysis revealed that variables such as catalyst dosage, sodium borohydride ($NaBH_4$) concentration, and reaction temperature had a pronounced influence on the conversion rate of 4-NP. Interestingly, Ag10@TAPP-COF also exhibited catalytic activity toward the reduction of other nitro-containing compounds, highlighting its versatility. Overall, this study introduces a promising pathway for designing robust and effective catalysts tailored for nitro compound reduction.

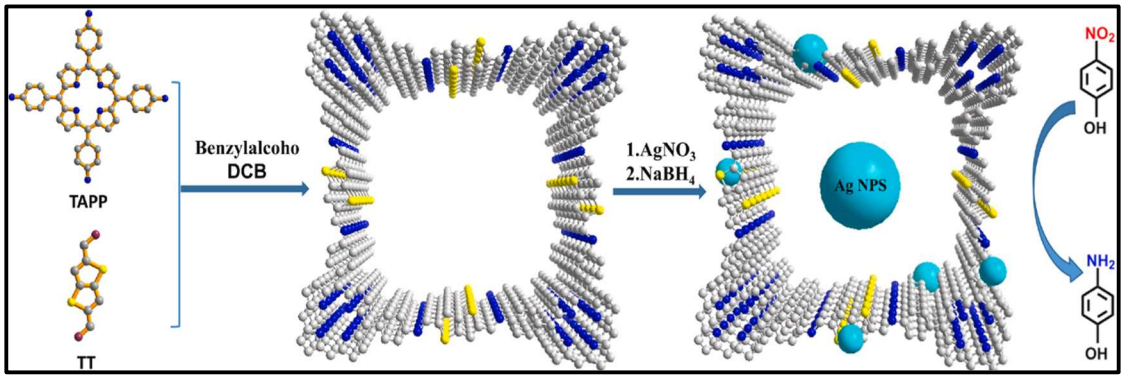

Fig.13: TAPP-TT-COF synthesis by encapsulating functionalised Ag(NPs). [29] [30]

1.5.1.2 COFs in metal-free catalysis:

i) Absorption of CO_2:

Their synthesized framework, designated as COF-609, was developed through a multi-step approach involving the initial formation of an imine-linked covalent organic framework, followed by post-synthetic modification and amine functionalization. The process began with the construction of a porous, crystalline COF via an imine condensation reaction between 2,4,6-tris(4-formylphenyl)-1,3,5-triazine (TFPT) and 4,4′-diaminobenzanilide (DABA), resulting in the intermediate COF-609-Im, represented by the reticular formula $[(TFPT)_2(DABA)_3]$imine. This crystallization was conducted in a solvent blend of mesitylene and n-butanol, using an aqueous acetic acid solution as a catalyst.

In the subsequent transformation step, COF-609-Im served as the starting material, wherein its imine bonds were chemically altered into tetrahydroquinoline (THQ) linkages through an aza-Diels–Alder reaction with 2-chloroethyl vinyl ether (CVE), facilitated by iron(III) ions (Fe^{3+}) in a diethyl ether medium. This conversion significantly enhanced the framework's chemical robustness, enabling it to tolerate strongly alkaline environments—a notable improvement over its imine-based counterpart.

Furthermore, the introduction of the −Cl moiety during this stage provided reactive sites for nucleophilic substitution. This enabled the incorporation of tris(3-aminopropyl)amine (TRPN) into the COF structure. [31] The modified framework was subsequently washed with a concentrated potassium hydroxide (KOH) solution to yield the final material: COF-609$\{[(TFPT)_2(DABA)_3$(-TRPN)x]THQ$\}$, which combines enhanced stability with functional versatility for advanced applications.

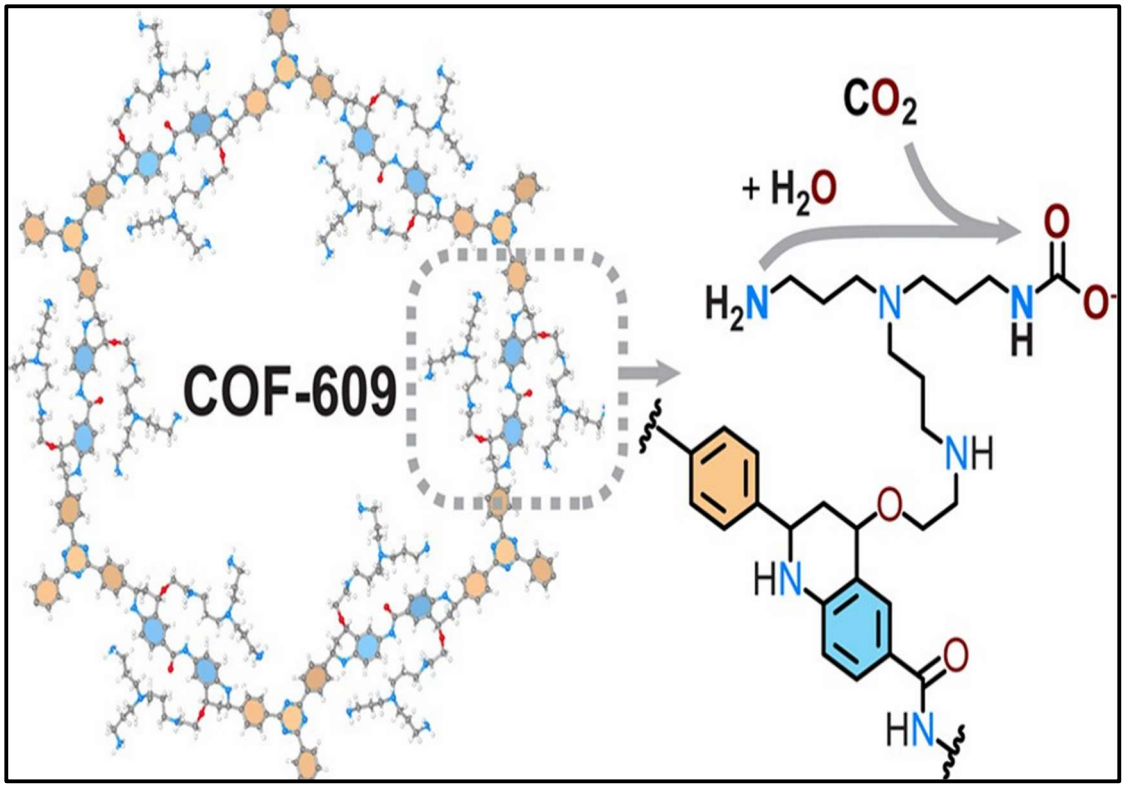

Fig.14: Schematic formation of COF-609 for CO2 capture. [32]

1.5.2 Photocatalytic and Electronic Applications of COFs:

Among the many functional uses of two-dimensional covalent organic frameworks (2D COFs), light-driven catalysis has surfaced as an especially promising and eco-conscious strategy for harnessing solar power and converting it into chemical energy to promote diverse organic conversions. These 2D materials, recognized for their porous architectures, absence of metals, and well-ordered polymeric crystalline structures, have increasingly attracted scientific interest for their photochemical potential.

Thanks to their advantageous attributes, 2D COFs have found widespread applications in crucial processes. [33] For instance, they play a significant role in photocatalytic water splitting, where solar radiation is employed to break water into hydrogen and oxygen—paving the way for clean, renewable hydrogen fuel production. In photoinduced redox processes, COFs act as facilitators for electron migration under light exposure, enabling a spectrum of chemical transformations. These frameworks have also exhibited strong capabilities in the selective photoreduction of carbon dioxide (CO_2) into high-value

chemicals—addressing both environmental sustainability and energy generation challenges.

Additionally, 2D COFs are capable of generating singlet oxygen, a reactive oxygen species widely used in synthesis and pollution control. Their utility extends to breaking down environmental contaminants via light-induced degradation, providing a powerful tool for pollution remediation.

Structural and Electrical Contributions of Layered COFs

The stacked sheet configuration of 2D COFs plays a critical part in preserving their stability and endowing them with distinctive electronic properties. Most of these frameworks adopt hexagonal or square-grid topologies, which offer a stiff, durable skeleton. The layered organization fosters robust interlayer π–π interactions, enhancing charge mobility across the framework. [34] These characteristics make them promising contenders for use in electrical energy storage (EES) systems.

Research teams, including Dichtel's group, have explored these applications extensively. A noteworthy example is the fabrication of thin films based on DAAQ-TFP COFs, which exhibit favorable properties for EES applications. These films can act as electrode materials or energy-storing units in supercapacitors and rechargeable batteries. Their strong π-orbital overlap and layered integrity are key to their effectiveness.

The performance of 2D COFs can also be enhanced by incorporating dopants—foreign atoms or molecules that alter their physical behavior. For instance, introducing iodine into FL-COF-1 has revealed its potential as a thermoelectric material. Thermoelectric can either generate electricity from excess heat or convert electrical energy into thermal energy. This dual functionality makes them ideal for energy recycling and waste heat recovery. By carefully tuning dopant concentrations and structural features, the energy conversion properties of COFs can be optimized for specific applications.

1.5.3 COFs in Drug Delivery Systems:

Covalent organic frameworks have emerged as a highly adaptable and efficient platform for drug delivery due to their customizable architecture, expansive surface area, and compatibility with biological environments. [35] Ongoing investigations continue to

expand their utility in medical treatments, improving their delivery efficiency and therapeutic potential.

Key Attributes Supporting Drug Delivery Applications:

Extensive Surface Area: The large surface coverage of COFs allows them to hold significant amounts of medicinal compounds, enabling potent doses to be carried effectively.

Tailored Porosity: Their tunable pore systems make it possible to accommodate a broad range of drug molecules, both small and large, and to release them in a regulated manner.

Architectural Flexibility: The framework structure of COFs can be engineered with specific pore dimensions and chemical groups, catering to different drug types and desired release profiles.

Chemical Resilience: These materials exhibit excellent chemical endurance in bodily fluids, making them reliable carriers for delivering medications without disintegration.

Biocompatibility: Many COFs are constructed from non-toxic organic constituents, ensuring minimal immune response and enhancing their safety for therapeutic use.

Mechanism of Drug Transport Using COFs:

Drug Encapsulation: Therapeutic agents can be embedded inside COF pores either by weak interactions (adsorption) or strong covalent linkages. [36] Their large internal surface and pore adaptability make them suitable for a range of molecules including proteins and genetic material.

Site-Specific Delivery: Functionalization with molecular targeting agents allows COFs to navigate toward particular tissues or diseased cells, such as tumors. This improves treatment accuracy while reducing damage to surrounding healthy tissues.

Controlled Dispersion: The drug release rate can be precisely regulated by modifying pore characteristics and chemical interactions within the COF, allowing for gradual and sustained therapeutic action.

Breakdown and Elimination: Post-delivery, COFs can be engineered to degrade into safe, non-toxic components that are easily expelled from the body, limiting long-term side effects.

Advantages in Therapeutic Delivery:

Extended Drug Life: Encasing drugs within COFs protects them from premature degradation by external factors, enhancing storage stability. [37]

Minimized Toxicity: By focusing drug delivery to targeted sites, COFs help reduce systemic side effects and improve patient comfort.

Enhanced Treatment Outcomes: Sustained and regulated release profiles support prolonged therapeutic effects, potentially reducing the frequency of medication doses.

CHAPTER-2

Synthesis and Characterization ST-COF and Fe@ST-COF

2. Synthesis and characterization of Fe loaded TAPP based COF:

2.1 Introduction of TAPP based COF:

Covalent organic frameworks (COFs) are a class of crystalline, porous materials constructed from organic building blocks linked through strong covalent bonds. Among the various linkers employed in COF synthesis, tetrakis(4-aminophenyl)porphyrin (TAPP) stands out due to its rigid planar structure, extended π-conjugation, and rich coordination chemistry. TAPP-based COFs have gained considerable attention because the porphyrin core not only contributes to structural stability and crystallinity but also imparts unique optical, electronic, and catalytic properties to the resulting frameworks. [38]

The porphyrin unit within TAPP is known for its excellent light-harvesting ability and strong affinity for metal coordination, which makes TAPP-based COFs promising platforms for applications in photocatalysis, sensing, and electrocatalysis. The incorporation of TAPP into COFs also facilitates the formation of well-defined channels and high surface areas, which are essential for guest molecule transport, adsorption, and active site accessibility in catalytic systems.

Moreover, the modular synthesis of TAPP-based COFs allows for tunable chemical functionality and pore environments, enabling their design for specific applications such as gas separation, pollutant degradation, and drug delivery. Due to their structural versatility and multifunctionality, TAPP-derived COFs represent a significant advancement in the development of functional porous materials tailored for sustainable chemical technologies.

TAPP-based COFs typically exhibit well-ordered mesoporous structures with pore sizes ranging from 1.5 to 3.5 nanometers, depending on the co-linker used. The tetratopic nature of TAPP forms extended 2D or 3D networks with uniform and tunable pore channels. By altering the geometry and length of the building blocks, the pore diameter can be precisely modulated. These pore sizes are ideal for hosting small molecules, metal nanoparticles, or catalytic species. High porosity and large surface areas (often exceeding 1000 m^2/g) enhance molecular accessibility. Such defined pore structures improve guest diffusion,

reaction kinetics, and size-selective catalysis. Hence, pore size in TAPP-based COFs plays a critical role in tailoring their functional applications.

***4,4'-(ethyne-1,2-diyl)dibenzaldehyde(SL-1):**

Structure: This compound consists of two benzaldehyde groups connected by an ethyne (-C≡C-) linker at the para-position (4,4'-position).

Functional Groups: Contains two aldehyde (-CHO) groups and a central alkyne bond, making it reactive for condensation reactions (e.g., Schiff base formation).

Synthesis Method: Typically synthesized via Sonogashira coupling between 4-iodobenzaldehyde and trimethylsilylacetylene, followed by desilylation using a base like K_2CO_3 in methanol.

Physical Appearance: Pale yellow to white crystalline solid.

Solubility: Soluble in organic solvents such as dichloromethane, ethanol, or THF.

Application: Used as a key building block in the synthesis of π-conjugated COFs, especially those that rely on aldehyde-amines for imine condensation.

***Meso-tetrakis(4-aminophenyl) porphyrin(TAPP):**

Structure: A porphyrin core with four para-aminophenyl groups at the meso positions (positions 5, 10, 15, and 20), offering four amino ($-NH_2$) functional sites for condensation reactions.

Functional Groups: Contains primary amines for Schiff-base (imine) formation and a conjugated porphyrin ring for optical and electronic activity.

Photophysical Properties: Exhibits strong UV-Vis absorption (Soret band ~420 nm; Q-bands ~500–700 nm), making it useful in photochemical and light-harvesting applications.

Solubility: Soluble in polar aprotic solvents like DMF, DMSO, and in acidic or basic aqueous solutions under certain conditions.

Thermal & Chemical Stability: High stability due to the rigid, aromatic porphyrin ring system, which resists thermal and oxidative degradation.

Applications: Used in COF synthesis (as a tetraamine linker).Catalysis (as a ligand for metal coordination).Photodynamic therapy, sensors, and optoelectronic devices due to its electron-rich and light-absorbing properties.

2.2 Experimental Section:

2.2.1 Material required for synthesis of TAPP:

All starting materials—4-nitrobenzaldehyde, pyrrole, propionic acid, and tin(II) chloride ($SnCl_2$),were obtained commercially and used without further purification. The resulting solid was isolated by filtration using a funnel. The final product was purified by recrystallization. Characterization was performed using FT-IR (KBr pellet method) and ^1H NMR (400 MHz) with DMSO-d_6 as solvent. Spectroscopic and analytical data supported the structure of the synthesized TAPP.

Procedure:

First, a chemical called 4-nitrobenzaldehyde 22 grams (1.45×10^{-1} mol) was mixed with acetic anhydride 24 mL (2.45×10^{-1} mol) and propionic acid which is 600ml in round bottom flask. Then, pyrrole 10 mL (1.45×10^{-1} mol) was slowly added to this mixture. After that mixture was refluxed for about 30 minutes, the mixture was cooled down, causing a solid to form. This solid was then filtered out, washed with water and methanol, and dried using a vacuum. Next, this dried powder was dissolved in more pyridine 160 mL and reflux for about an hour. After it was cooled down, another solid formed. This was again filtered, washed with acetone, and a purple crystal (called R-NO_2) was obtained with a 14% yield. After that, around 4.13 gm (9.2×10^{-3} mol) of this crystal was dissolved in hot hydrochloric acid (HCl) which is 500mL at 70°C. Tin chloride Dihydrate ($SnCl_2.2H_2O$) which is 18 gm (7.97×10^{-2} mol) was added to the solution and the mixture was reflux for 30 minutes at the same temperature. It was then allowed to cool to room temperature. Ammonia (NH_3) was used to neutralize the solution, which caused a gray solid to form. This was filtered, dissolved in acetone, and then dried using a vacuum to finally give the desired purple crystals. (Scheme.1)

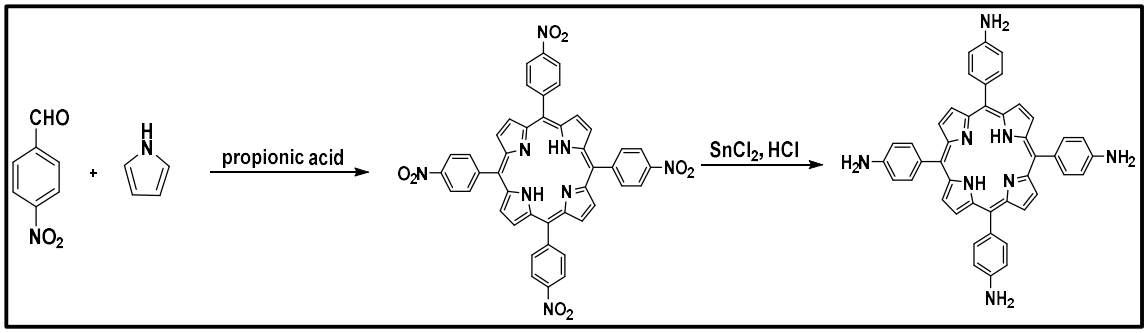

Scheme.1:-Synthesis of meso-tetrakis(4-aminophenyl) porphyrin (TAPP)

2.2.2 Material required for synthesis of SL-1:

All the starting chemicals—4-bromobenzaldehyde, 4-ethynylbenzaldehyde, copper(I) iodide (CuI), triethylamine (NEt_3) as the base, Bis(triphenylphosphine)palladium chloride ($PdCl_2(PPh_3)_2$), and tetrahydrofuran (THF) as the solvent—were bought from suppliers and used directly without any extra cleaning or processing. The solid material that formed during the reaction was purified by Column chromatography. To confirm what was made, tests were done using FT-IR (with the KBr pellet method) and proton NMR spectroscopy (^{1}H NMR at 400 MHz), using DMSO-d_6 as the liquid to dissolve the sample. The results from these tests supported that the desired compound, SL-1, was successfully made.

Procedure:

To start, all the materials were handled in an environment where oxygen was removed (using nitrogen gas). First, 4-bromobenzaldehyde 675 mg (3.65mmol,1eq) and 4-ethynylbenzaldehyde 475 mg (0.05 eq) were mixed together with a small amount of copper iodide 35 mg (183.4 mol, 0.05 eq) in 50 milliliters of dry THF in round bottom flask. To make sure no moisture or air got in, the flask was filled with nitrogen gas and kept sealed. After that, dry triethylamine 7.3 mL (52.3mmol, 14.0 eq) was added slowly with a syringe, which caused the color of the solution to turn dark brown. The mixture was stirred at room temperature for about 16 hours. Once the reaction was finished, the extra solvent were removed under reduced pressure. The remaining material was cleaned up using a method called column chromatography with a mixture of dichloromethane and hexane (in a 5:1 ratio) as the liquid to carry the compounds through the column chromatography.

This process gave white crystals (556 mg), which corresponds to a 88% yield. The amount of palladium catalyst used in the reaction was around 64 mg, which equals 183.9 micromoles (0.05 eq).

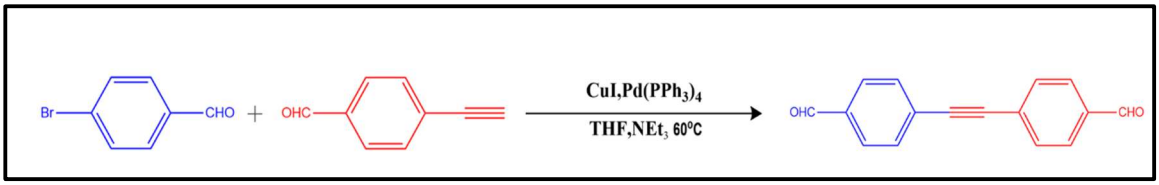

Scheme.2:-Synthesis of 4,4'-(ethyne-1,2-diyl)dibenzaldehyde(Sonogashira Coupling).

2.2.3 Material required for synthesis of ST-COF:

All the chemicals used in the synthesis of the ST-COF were obtained from above synthesis and used with further purification. The key reactants included meso-tetrakis(4-aminophenyl) porphyrin (TAPP) and 4,4'-(ethyne-1,2-diyl)dibenzaldehyde (SL-1). The condensation reaction was carried out using o-dichlorobenzene (o-DCB) and n-butanol as the solvent system, with acetic acid serving as the catalyst. After the reaction, the resulting material was thoroughly washed with N,N-dimethylformamide (DMF) and tetrahydrofuran (THF) to remove unreacted residues and by-products.

Procedure:

For the synthesis of the ST-COF, the key starting materials used were meso-tetrakis(4-aminophenyl)porphyrin (TAPP), weighing 157 mg (0.33 mmol), and 4,4'-(ethyne-1,2-diyl)dibenzaldehyde (SL-1), weighing 227 mg (0.67 mmol). The reaction was carried out in a mixture of 8.25 mL of o-dichlorobenzene (o-DCB) and 2.75 mL of n-butanol as solvents. To facilitate the condensation reaction, 500 µL of 6 M acetic acid was added as a catalyst. The mixture was placed in a sealed pressure tube and heated at 120°C for 72 hours. After completion of the reaction, the solid product formed was thoroughly washed several times with N,N-dimethylformamide (DMF) and tetrahydrofuran (THF) to remove any unreacted materials and impurities. Finally, the product was dried at 80°C, yielding a purple solid with an overall yield of approximately 62%.

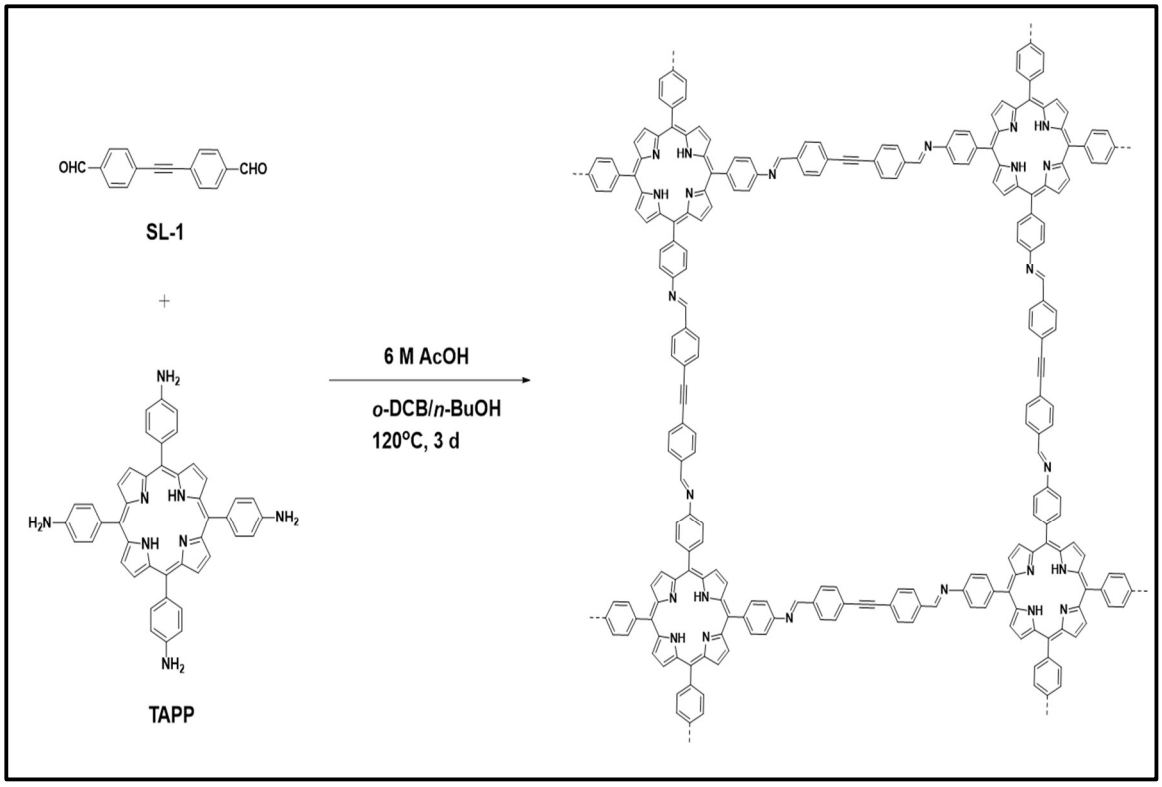

Scheme.3:- Synthesis of ST-COF

2.2.4 Synthesis of Iron(III) loaded COF as a Fe@ST-COF:

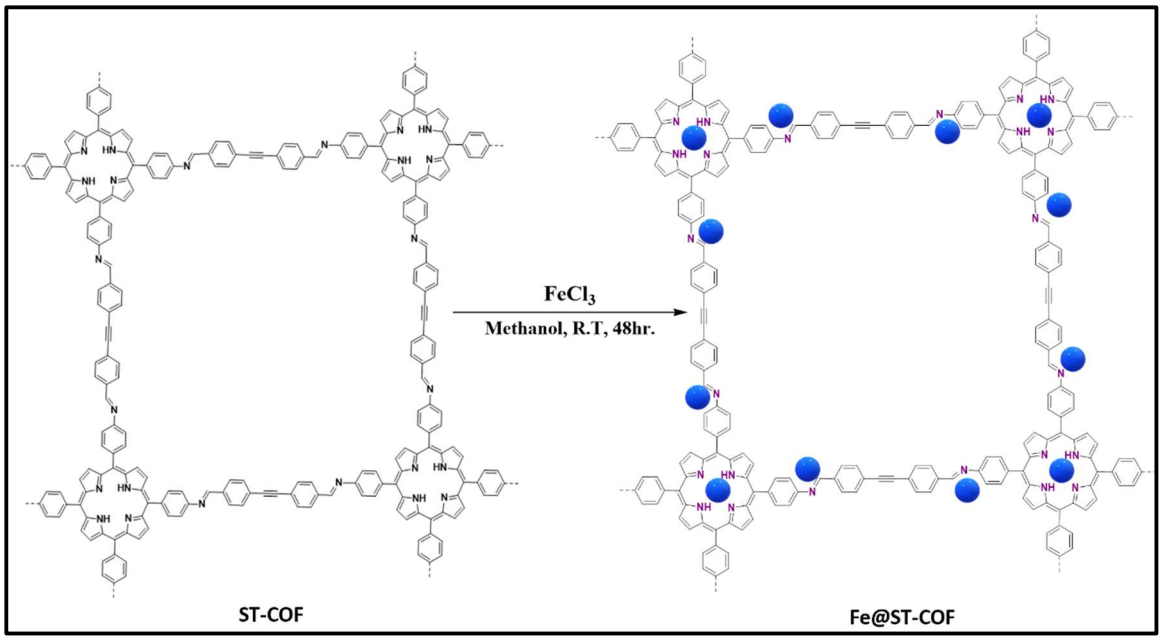

Scheme.4:- Synthesis of iron loaded Fe@ST-COF

To prepare the ST-COF material, 100 mg of ST-COF powder was first mixed with methanol in a flask and stirred gently for about 10 minutes to help it disperse evenly. Then,

270 mg of dry iron chloride ($FeCl_3$), also dissolved in methanol, was mixed. This mixture was stirred continuously for 48 hours at room temperature so the iron could attach properly. After the process, the material was washed with methnol to remove any leftover chemicals and dried in an oven. The final iron-loaded ST-COF was then examined using FT-IR to check its chemical bonds, XRD to see how orderly its structure was, and BET analysis to measure its surface area and pore size.

2.3 Characterization of SL-1, TAPP, ST-COF and Fe@ST-COF:

2.3.1 FT-IR study of TAPP:

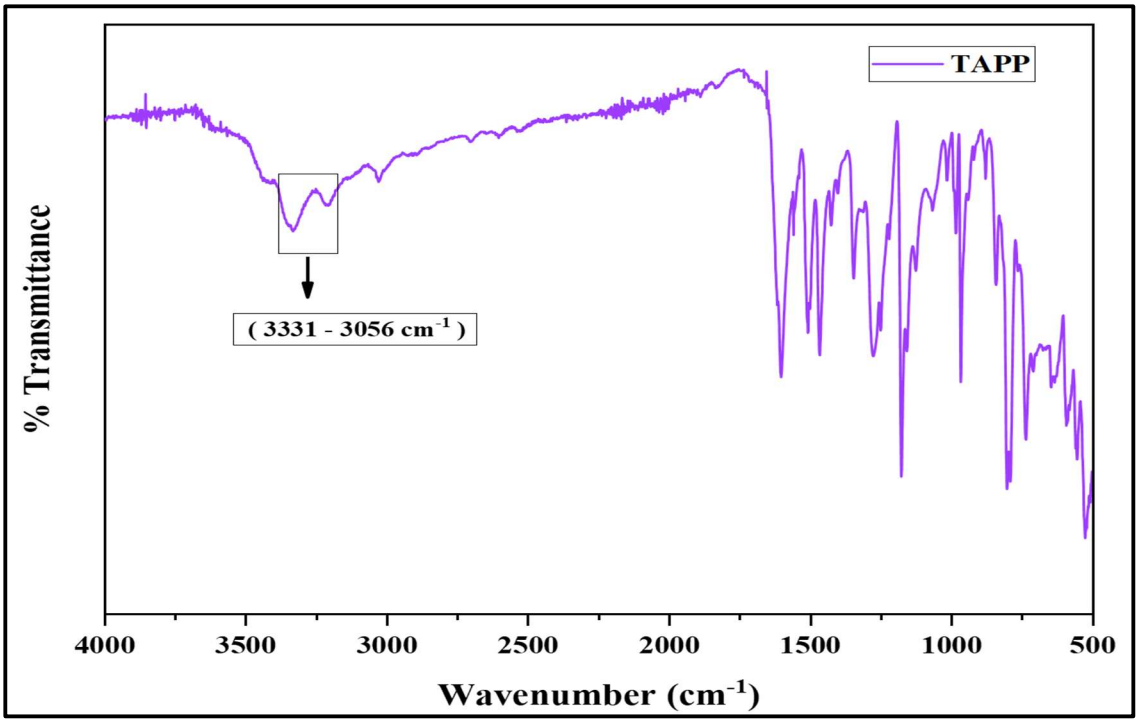

Fig.15-FT-IR analysis of TAPP

The FT-IR spectrum of TAPP shows several important peaks that help confirm the structure of the molecule in the above **Fig.15**. A broad peak around 3300 cm^{-1} is due to N–H stretching, which comes from the amine ($-NH_2$) groups in the structure. Just above 3000 cm^{-1}, there is a peak indicating the presence of C–H stretching in aromatic rings. Peaks around 1600 cm^{-1} and 1500 cm^{-1} correspond to C=C stretching, which is typical for the benzene rings in the porphyrin core. A peak near 1350–1400 cm^{-1} is related to C–N stretching, confirming the amine linkage. Below 1000 cm^{-1}, multiple peaks are seen, which are due to C–H bending in the aromatic system and out-of-plane deformation vibrations.

Altogether, these peaks confirm that TAPP contains aromatic rings, amino groups, and the expected molecular structure.

2.3.2 Comparative FT-IR analysis of synthesized Compounds:

In the **Fig.16** SL-1 starting material, we can see a strong peak around 1702 cm^{-1}, which is a sign of a C=O (carbonyl) bond. However, this peak is not seen in the TAPP sample, as expected. After the reaction, in the ST-COF sample, the C=O peak disappears, and a new peak appears around 1623 cm^{-1}, which is related to a C=N (carbon-nitrogen double bond). This shows that the chemical reaction worked and the COF was formed properly. In the final Fe@ST-COF material, there is still no C=O peak, and the C=N peak remains, confirming the structure is stable. Additionally, some new peaks appear in the fingerprint region around 500–700 cm^{-1}, which are signs of Fe–N (iron-nitrogen) bonds. These peaks together confirm that the COF was correctly synthesized and that iron was successfully incorporated into the structure.

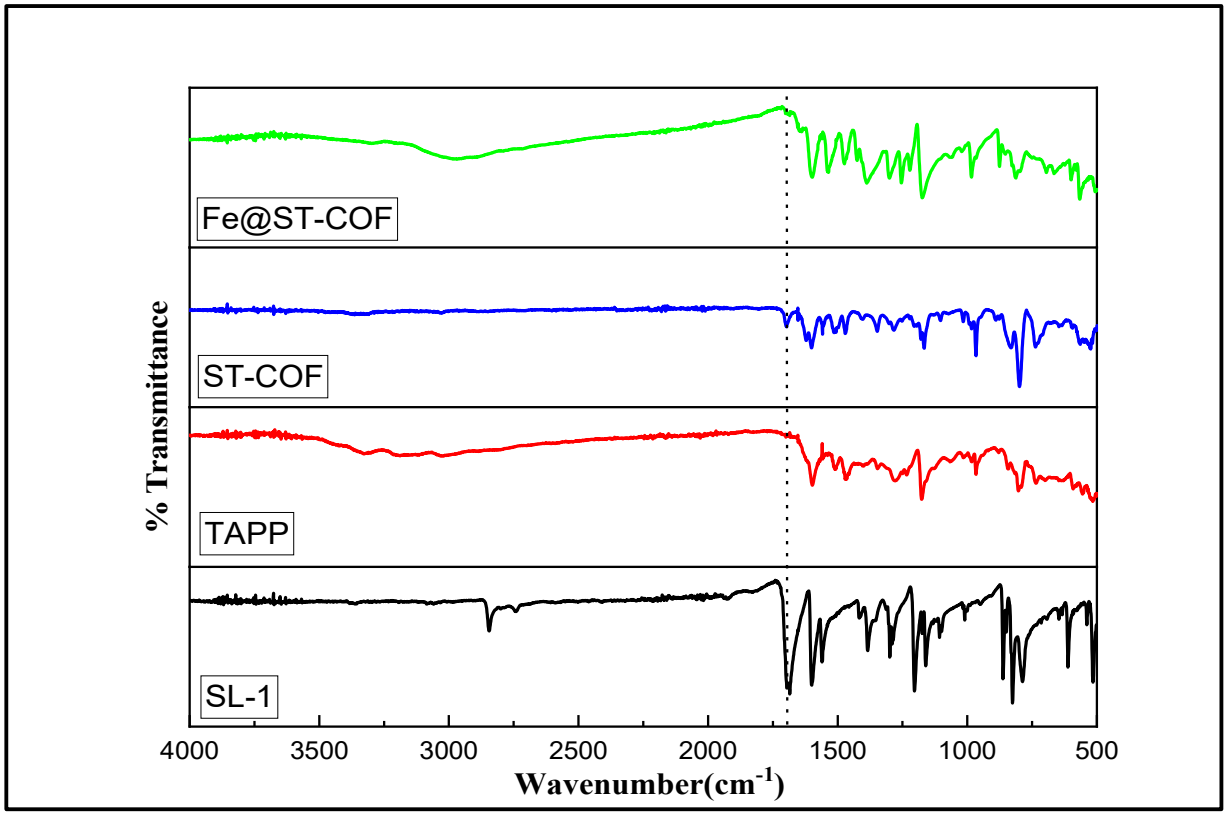

Fig.16- FTIR of SL-1,TAPP,ST-COF and Fe@ST-COF.

2.3.3 XRD Analysis:

In the XRD graph(**Fig.17**), we can see how the structure of the materials changes. The SL-1and TAPP linker show shap peaks at 11.2° , 24.3°, 26.2°, and 21.1°, which means these materials have a well-ordered, crystal-like structure. When these two are combined to make ST-COF, we still see a clear peak around 21.7°, showing that the structure is converted poly-morphous. But when iron (Fe) is added to form Fe@ST-COF, those sharp peaks become broader and less clear, and we notice two wide bumps at around 35.6° and 54.5°. These bumps match with known patterns of iron chloride ($FeCl_3$), so we can tell that iron has successfully attached to the COF. However, because the peaks are no longer sharp, it also tells us that the structure has become, a bit more amorphous. After loading the iron the structure of the ST-COF remains intact. So overall, this confirms that iron has been successfully immobilized on ST-COF.

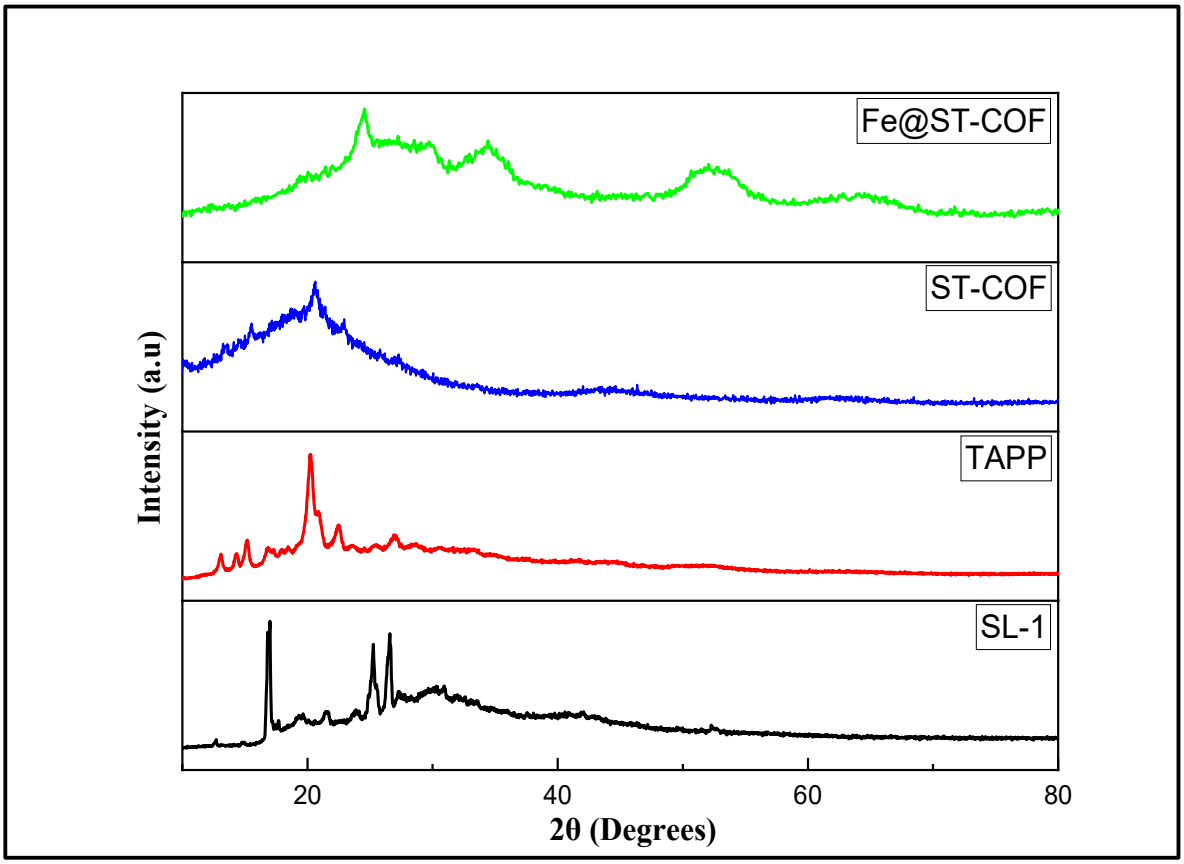

Fig.17-PXRD of TAPP, SL 1,ST-COF and Fe@ST-COF

2.3.4 TGA analysis of ST-COF and Fe@ST-COF:

The TGA (Thermogravimetric Analysis) graph(**Fig.18**) helps us understand how stable two materials — ST-COF and Fe@ST-COF — are when heated. As temperature increases, the materials slowly start to lose weight, which tells us how much of the material is breaking down. The black line represents ST-COF, and the red line represents Fe@ST-COF (which has iron added). TGA was carried out using a temperature range of 50-800°C. The intial weigt loss at 90 to 100°C indicates desorption of trapped solvents and moistures. The TAPP porphyrin core and the framework eventually decomposes at 505.92°C (94.25%). Even at 587.73°C, it still holds on to 78.06% of its original weight. This confirms that ST-COF is thermally stable upto 505.92°C. On the other hand, Fe@ST-COF starts to lose weight a bit earlier. At 491.91°C, it keeps 81.28% of its weight, and at 545.62°C, it retains only 73.55%. This means that adding iron makes the material a little less heat-resistant. Overall, both materials show good thermal stability, but the original ST-COF performs slightly better when exposed to high heat.

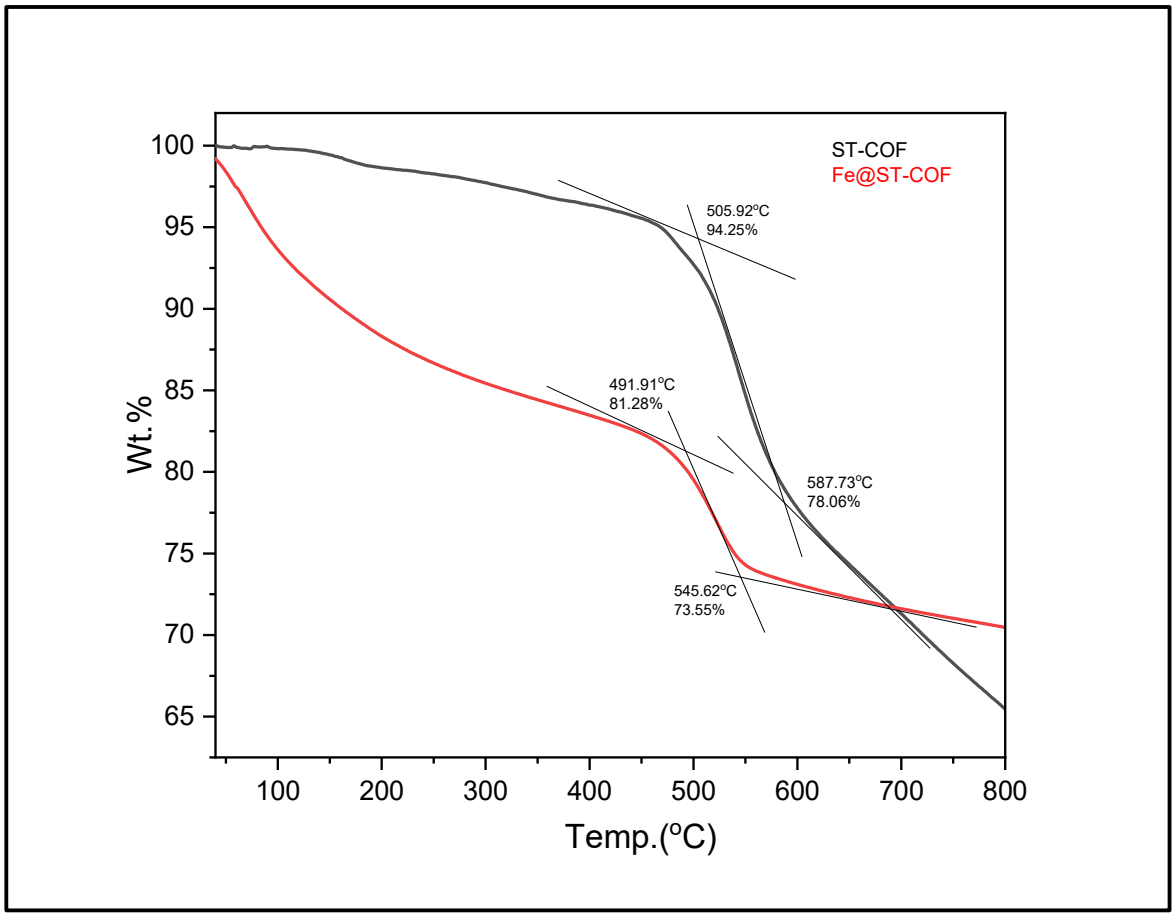

Fig.18-TGA analysis of ST-COF and Fe@ST-COF

2.3.5 BET analysis of ST-COF:

A nitrogen gas adsorption-desorption curve was employed to analyse the surface area and porosity of the ST-COF catalyst. The BET (Brunauer–Emmett–Teller)(**Fig.19**) method was used to calculate these values. According to the results, the surface area of ST-COF was found to be 65.3769 m^2/g, indicating a good amount of surface available for reactions. The pore volume was measured to be 0.08945 cc/g, showing the total amount of space available inside the pores. Additionally, the average pore radius was calculated to be 1.6286 nm, confirming that ST-COF has a mesoporous structure. These features suggest that ST-COF can be effective for applications such as adsorption, catalysis, or gas storage.

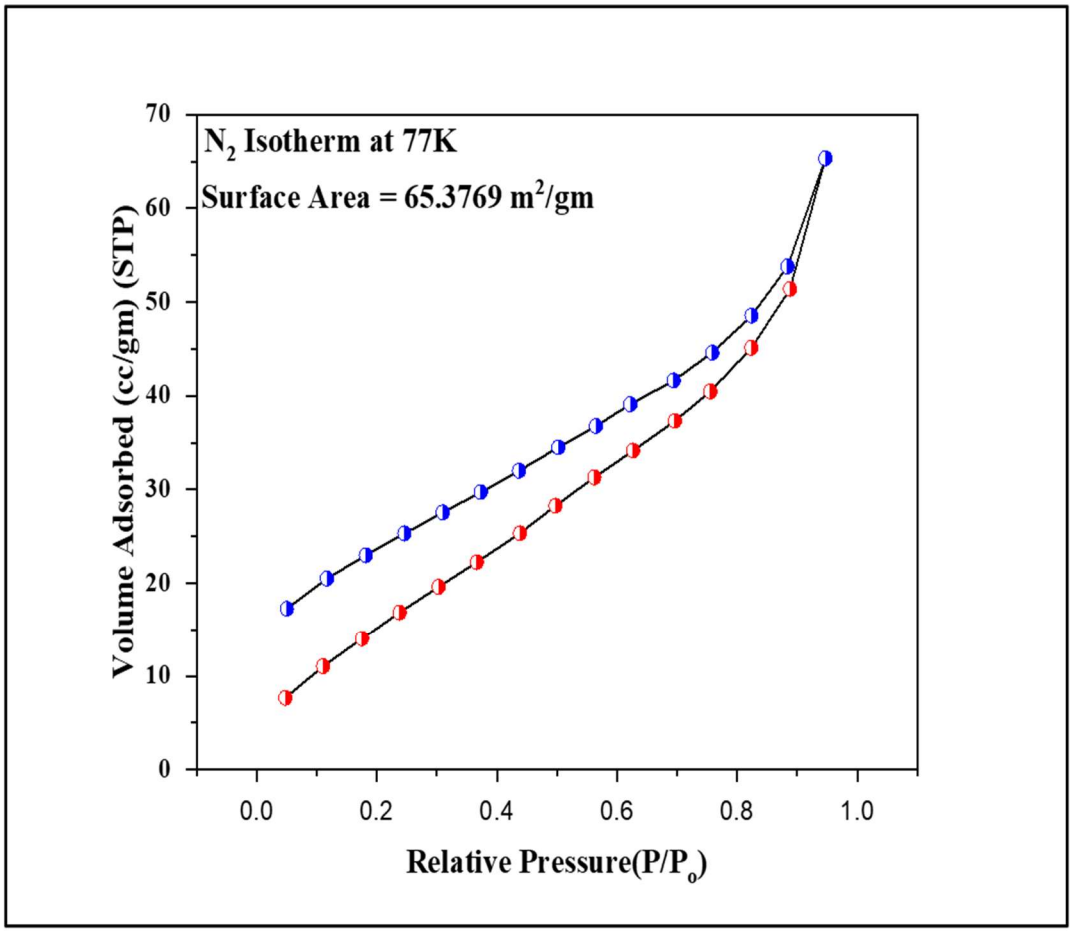

Fig.19-Nitrogen sorption isotherm of ST-COF

2.3.6 XPS analysis of Fe@ST-COF:

X-ray Photoelectron Spectroscopy (XPS) (**Fig.20**) analysis was carried out to confirm the presence and chemical state of iron (Fe) in the Fe@ST-COF material. In the Fe 2p spectrum, two main peaks are observed — one at 711.2 eV, corresponding to Fe $2p_{3/2}$, and another at 724.4 eV, corresponding to Fe $2p_{1/2}$. These peak positions indicate that iron is present in the Fe^{3+} oxidation state, which is typical for iron species such as $FeCl_3$. The appearance of these peaks confirms that iron has been successfully incorporated into the ST-COF framework. Additionally, the satellite peaks further support the oxidation state and proper chemical environment of Fe in the composite material.

An X-ray Photoelectron Spectroscopy (XPS) survey scan was conducted on Fe@ST-COF to identify all the elements present on its surface. The spectrum clearly shows peaks corresponding to carbon (C 1s) around 284.8 eV, nitrogen (N 1s) near 399.8 eV, and oxygen (O 1s) at 531.7 eV, indicating the presence of organic linkers and functional groups in the structure. Most importantly, a distinct peak for iron (Fe 2p) appears near 711.2 eV, confirming the successful incorporation of iron into the framework. These results confirm that Fe@ST-COF contains the expected elements, supporting its formation as a metal-incorporated covalent organic framework (COF). The overall elemental composition proves that iron is evenly distributed and well-integrated with the COF material.

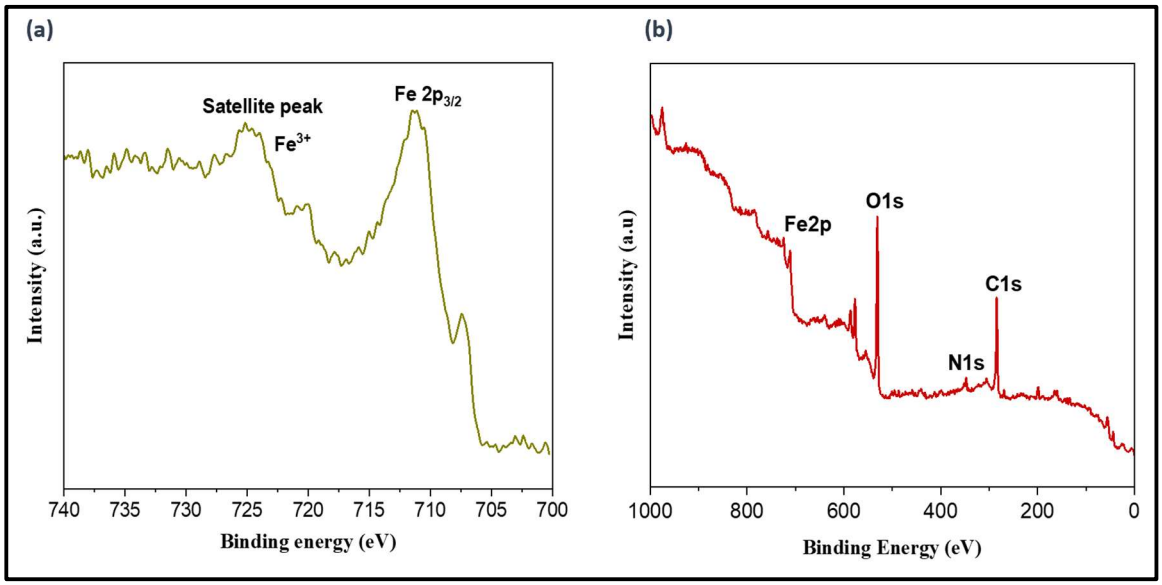

Fig.20-(a) Fe2p spectra and (b) Full elemental survey spectra of Fe@ST-COF.

2.3.7 FESEM results of ST-COF(Fig.21):

Morphology: The SEM images reveal that ST-COF possesses a predominantly spherical morphology, forming aggregated clusters with interconnected structures. Particle Shape: The particles are uniformly spherical to semi-spherical, indicating a consistent and controlled synthesis process. Particle Size: The particle diameters range from 289 nm to 399 nm, based on the high-magnification image annotations, suggesting a narrow size distribution. Surface Texture: The surface of the particles appears rough and porous, which is advantageous for catalytic and adsorption applications due to enhanced surface area. Aggregation: The particles are loosely aggregated, forming a sponge-like, porous network, which may facilitate efficient diffusion of reactants. Crystallinity Indication: The defined shapes and surface features imply a degree of crystallinity or structural regularity in the material.

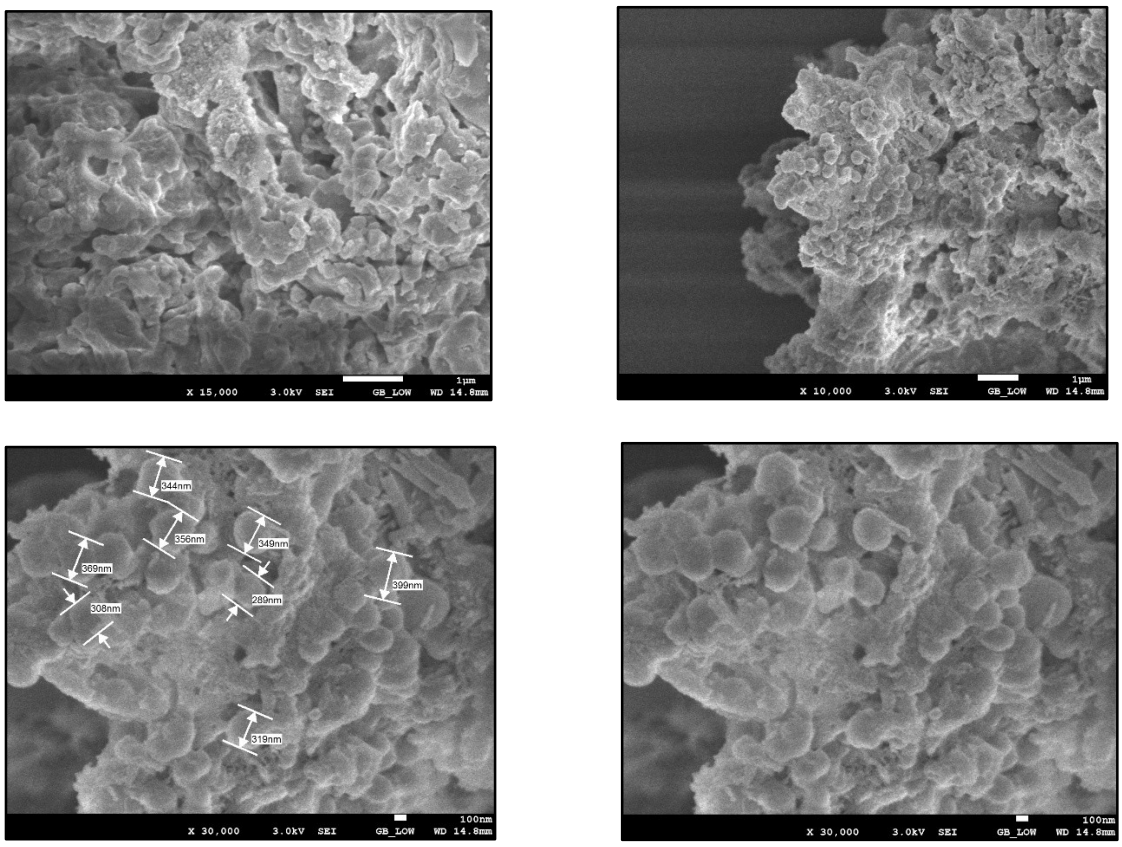

Fig.21-FE-SEM Images of ST-COF

2.3.8 FESEM results of Fe@ST-COF(Fig.22):

Surface Texture: The surface appears rougher and more uneven than the plain ST-COF. This is likely due to tiny iron (Fe) particles attaching themselves to the COF, making it look bumpier. Particle Shape: The general spherical or rounded shape of the COF is still visible. However, the surface is no longer smooth — instead, it's covered with small irregular clusters. Size Distribution: The particles show a wider range in size — some are large clumps while others are small grains. This difference in size may be because iron particles have grouped together in some areas. Evidence of Iron Presence: In comparison to plain ST-COF, you can now see extra features on the surface — small blobs or clusters. These are not seen in the unloaded COF and confirm that iron has been successfully added to the structure.

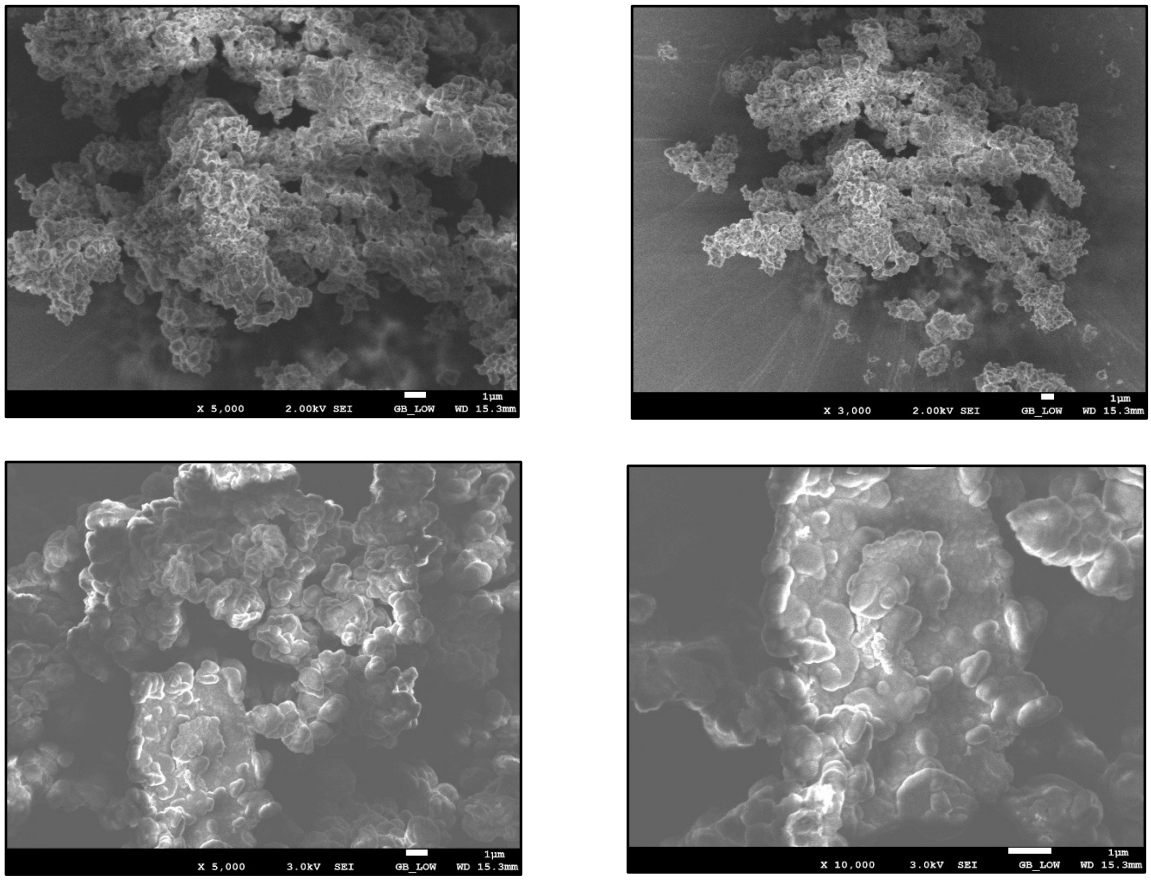

Fig.22-FE-SEM Images of Fe@ST-COF

2.3.9 EDS analysis and Elemental Mapping:

(1). ST-COF(Fig.23)

Main Elements Detected: Carbon (C): ~***75.7*** wt.% Nitrogen (N): ~***24.3*** wt.% Oxygen (O): Not detected in this scan (expected due to imine linkage, not polyimide).What This Tells Us: The high carbon content makes sense because the COF is made from organic building blocks (TAPP and SL-1). The presence of nitrogen is strong evidence for imine (–C=N–) linkages, which are formed when amines react with aldehydes (as in TAPP + SL-1 reaction). The absence of oxygen aligns with the fact that this is not a polyimide (which would contain significant oxygen). Conclusion: The EDS data confirms the presence of carbon and nitrogen in the expected ratios. These results support the successful formation of an imine-based COF structure, consistent with the chemistry of the TAPP-SL1 reaction.

(2). Iron-loaded as Fe@ST-COF(Fig.24)

Carbon (C) – ***77.9*** wt.%. The high carbon content confirms the presence of the organic framework (ST-COF), which is primarily composed of carbon-rich components like TAPP and SL-1. Nitrogen (N) – ***16.3*** wt.%. Nitrogen is a key element in the imine (-C=N-) linkages, indicating that the structural integrity of the COF is maintained after iron loading. Iron (Fe) – ***5.8*** wt.%. The appearance of distinct iron peaks confirms that Fe has been successfully introduced into the COF structure. This verifies the formation of Fe@ST-COF. Presence of Iron Peaks: The spectrum clearly shows Fe Kα and Kβ peaks (~6.4 keV and ~7.0 keV), which are not present in the pristine ST-COF, confirming iron incorporation. No Unexpected Elements: The spectrum shows only the expected elements (C, N, Fe), indicating a clean synthesis without unwanted contaminants.

(a)

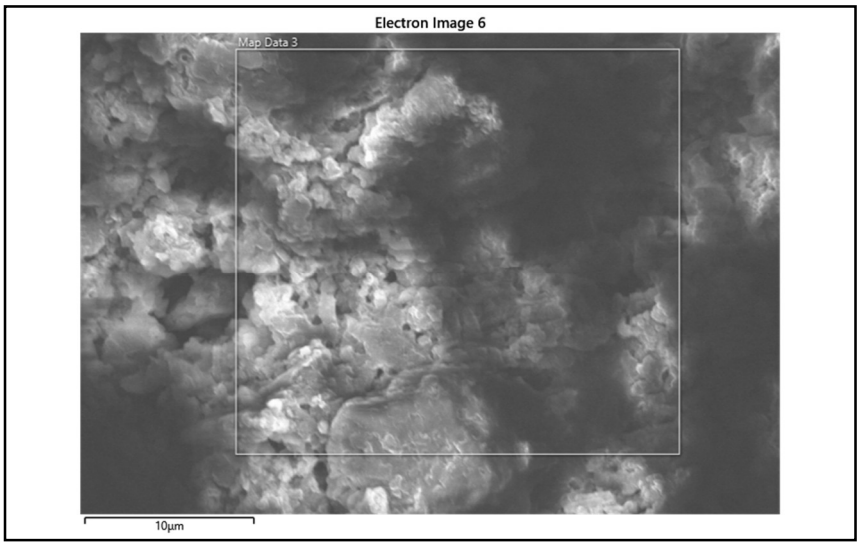

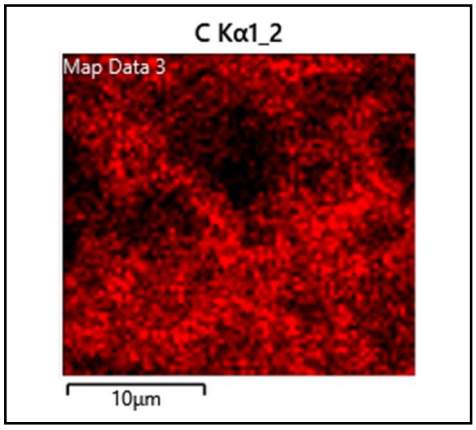

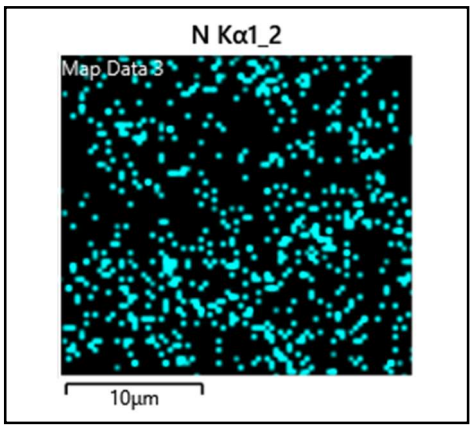

(b)

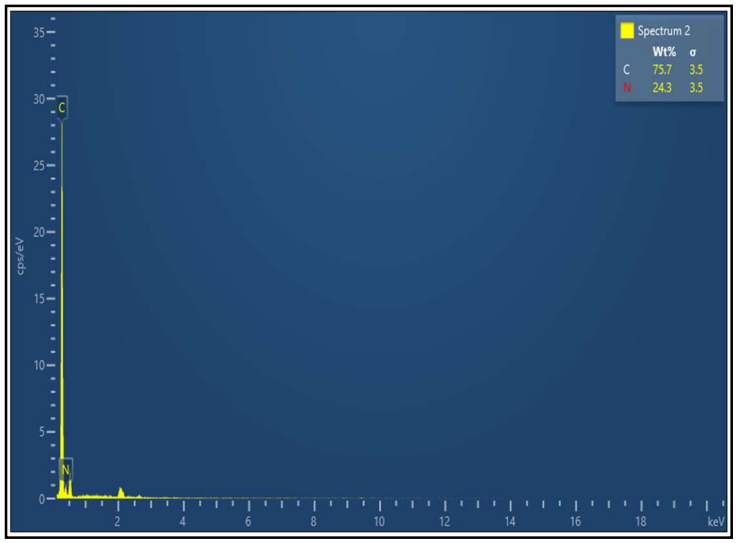

Fig.23-ST-COF (a) Elemental mapping and (b) SEM-EDS analysis

(a)

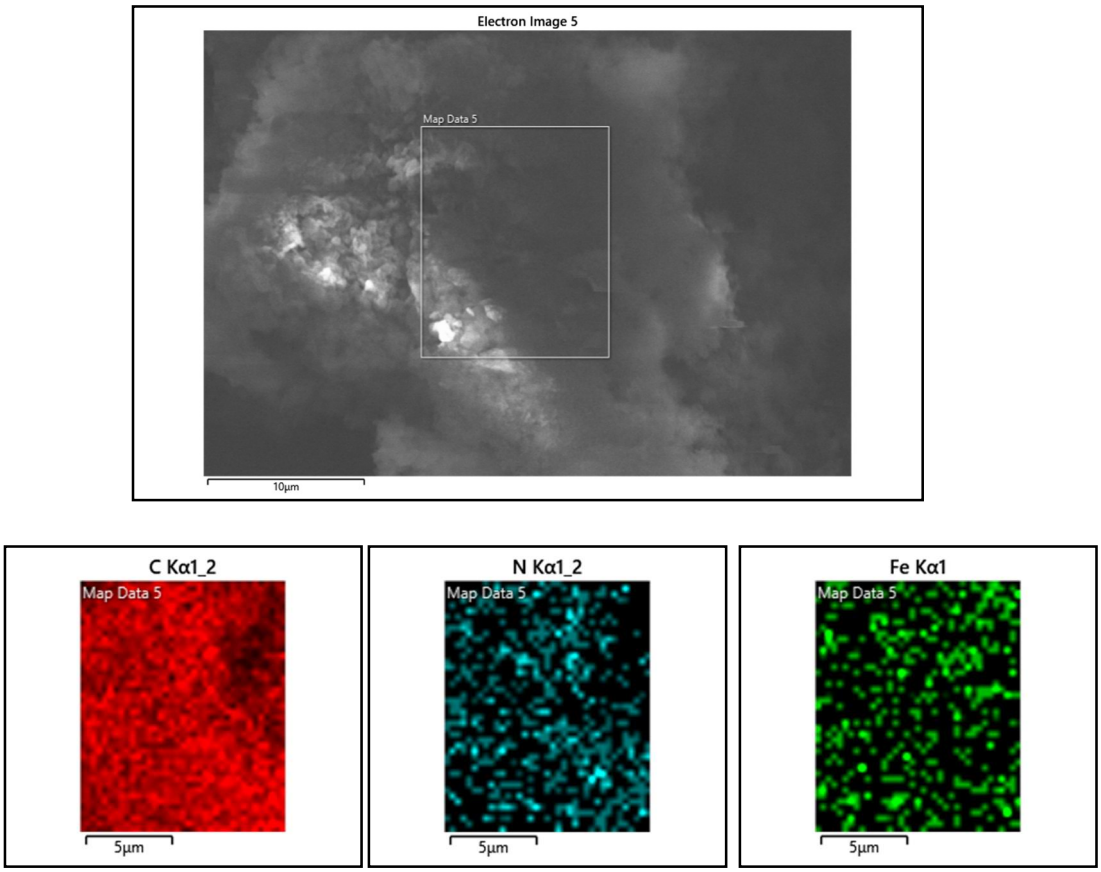

(b)

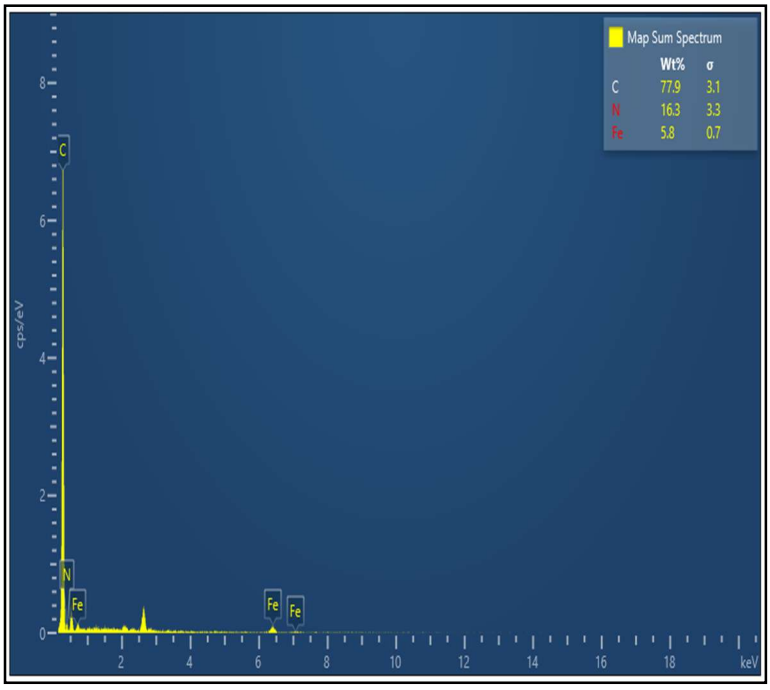

Fig.24-Fe@ST-COF (a) Elemental mapping and (b) SEM-EDS analysis

***NMR Spectral Data:**

(1). ^{1}H NMR of 4,4'-(ethyne-1,2-diyl)dibenzaldehyde

^{1}H NMR (400 MHz, $CDCl_3$): δ 9.96 (s, 2H), 7.89 (d, J = 8.4 Hz, 4H), 7.43 (d, J = 8.4 Hz, 4H)

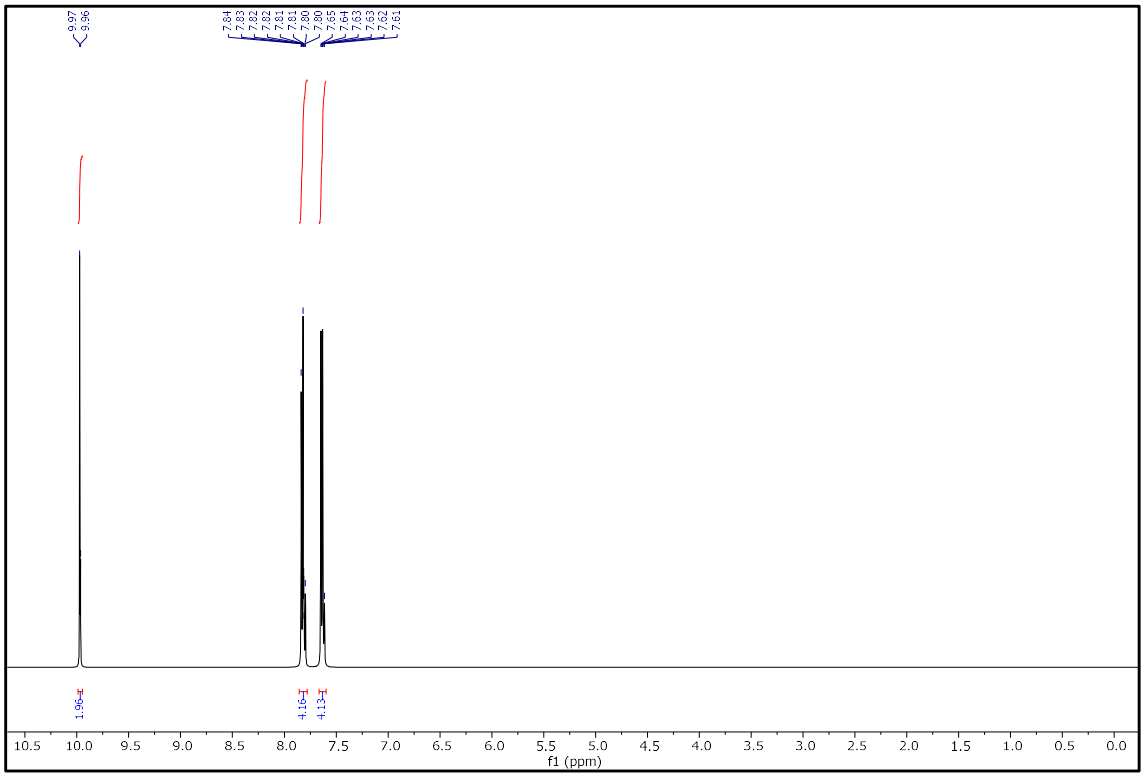

CHAPTER-3

Catalytic application using Fe@ST-COF as an Efficient Catalysts for synthesis of polysubstituted pyridine

3. Catalytic application of Fe@ST-COF as a heterogeneous catalyst for synthesis of poly-substituted pyridine:

3.1 Introduction to multicomponent reaction for synthesis of pyridine and their uses:

1. Introduction

Pyridine is a special kind of chemical ring that contains nitrogen. It plays an important role in many things we use daily, including medicines, dyes, and even materials used in technology. Because it has a nitrogen atom in its ring, pyridine behaves differently from other rings made only of carbon, giving it unique powers—like easily attaching to other atoms or forming strong, stable structures. Scientists are very interested in making new versions of pyridine for health and industry. To do that, they need ways to build these molecules quickly, affordably, and without harming the environment. Recent research has focused on green and efficient methods using fewer steps and cleaner chemicals. Two important studies help us understand this better—Islam et al. (2023) [39] reviewed the many ways to make pyridine, while Wu et al. (2014) showed a clever way to make complicated pyridine molecules using a simple iron salt.

2. Why Pyridine is Important

Pyridine's structure gives it superpowers in chemistry. Its nitrogen atom makes it easy to change, add to, or connect with other chemicals. [40] [41] This is why it shows up so often in useful products. In medicine, pyridine is part of many drugs. It can help the medicine stay in the body longer or stick better to its target. For example, drugs like nicotinamide (a vitamin), isoniazid (used for tuberculosis), and roflumilast (for lung problems) all contain pyridine. [42]

But it's not just about medicine—pyridine is also used in farm chemicals, dyes, and even in materials that store gases or conduct electricity. [43] Because of how flexible and powerful it is, chemists often use pyridine as a "starting block" to build more complex chemicals. [44]

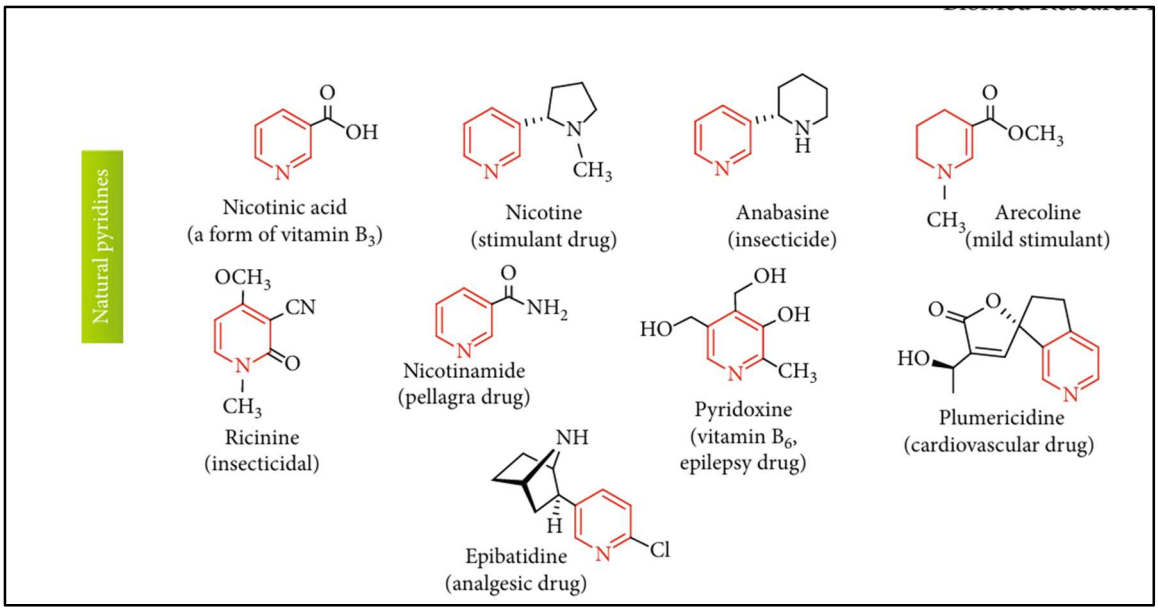

Fig.25:- Picture of some natural polysubstituted pyridine

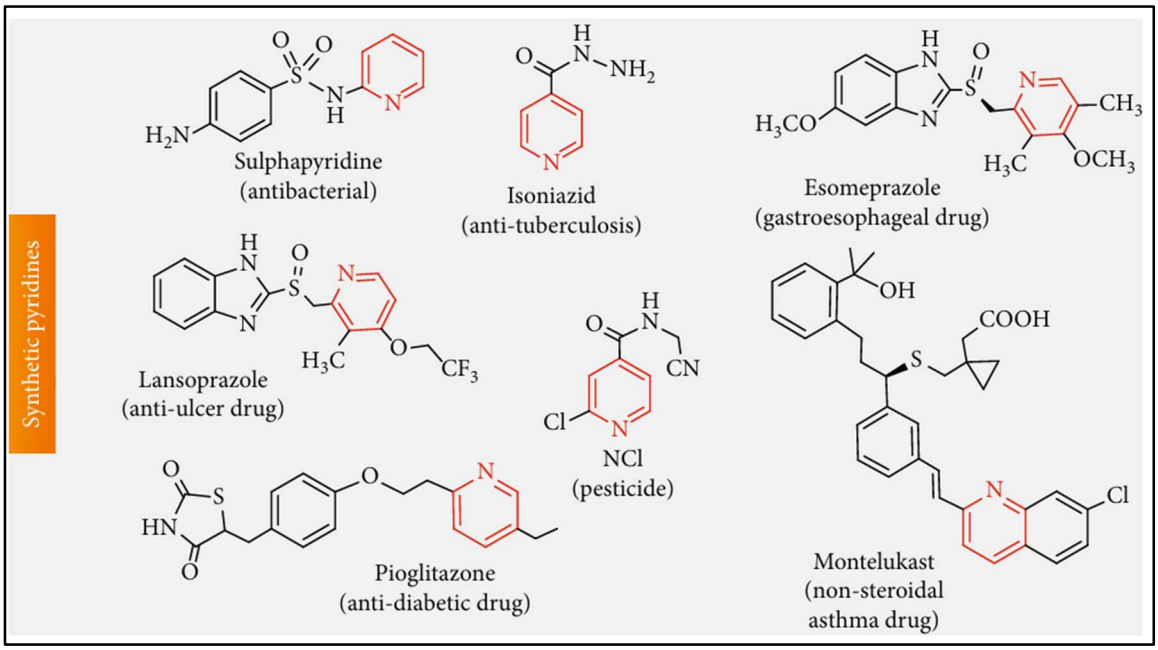

Fig.26:- Picture of some synthetic polysubstituted pyridine.

3. Old and New Ways to Make Pyridine

People have been making pyridine for over 100 years using some classic methods, like the Hantzsch reaction and Chichibabin reaction. [45] [46] These methods work, but they can be messy—they use harsh chemicals, create waste, and sometimes require many steps.

Today, scientists prefer cleaner, faster methods that use fewer chemicals and are better for the planet. Some of the best new ways involve metal catalysts like palladium, nickel, or copper. These metals help reactions happen faster and make it easier to add different chemical groups to the pyridine ring. [47]

There are also newer ways that don't even need metals. These use tiny organic molecules (called organocatalysts) that can do the same job. These are better for health and the environment since they don't leave behind metal waste. [48]

4. Multicomponent Reactions and Green Chemistry

A really exciting development is the use of multicomponent reactions, or MCRs for short. These are like cooking everything in one pot—you toss in different ingredients, and they all react together at once. [49] This saves time, cuts down on waste, and is great for making complex molecules like pyridine quickly. Wu et al. (2014) created a smart recipe using iron chloride ($FeCl_3$), which is cheap and safe. They mixed four simple chemicals together in one step and made complex pyridine compounds. It was fast, clean, and worked really well. Iron is also more eco-friendly than precious metals like gold or platinum. [50]

Meanwhile, Islam et al. (2023) looked at even more tools to make pyridine, like using microwave heating (like fast cooking), flow chemistry (like chemistry on a conveyor belt), and green solvents (liquids that don't harm the environment). These techniques make the whole process even better for industrial use.

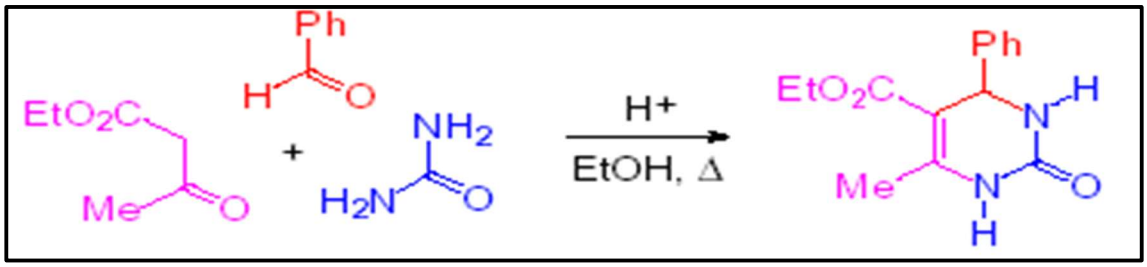

Fig.27:-Synthesis of DHPM via Biginelli Reaction. [51]

5. What Pyridine Can Be Used For

Pyridine-based chemicals are like superheroes—they can do many things. In medicine, they fight bacteria, cancer, inflammation, and viruses. They're strong, stable, and good at fitting into tiny pockets in proteins, which is what you want in a good drug .Outside of medicine, pyridine is used in electronics, solar cells, and materials that can hold gases like

hydrogen or carbon dioxide. These are useful in clean energy and environmental protection. Pyridine is also part of some powerful weed killers and bug sprays used in farming, like paraquat and diquat.

3.2 Results and Discussion:

A four-component condensation reaction involving 4-nitrobenzaldehyde, methyl acetoacetate, aniline, and malononitrile was carried out under optimized conditions using Fe@ST-COF as a catalyst. This approach led to the successful synthesis of a highly substituted pyridine derivative, namely methyl 5-cyano-2-methyl-4-(4-nitrophenyl)-6-(phenylamino)nicotinate, in good yield. The reaction proceeded smoothly under mild conditions, highlighting the effectiveness of the Fe@ST-COF catalyst in facilitating the construction of the polysubstituted pyridine ring. The successful formation of this complex molecule underlines the potential of this catalytic system in enabling multicomponent reactions for the efficient synthesis of functionalized heterocycles. The reaction showcases good atom economy and aligns well with green chemistry principles by utilizing an iron-based, non-toxic catalyst. The proposed mechanism for this transformation is illustrated in Figure 27 , providing insights into the stepwise formation of the nicotinate framework. Considering it to be fast reaction.

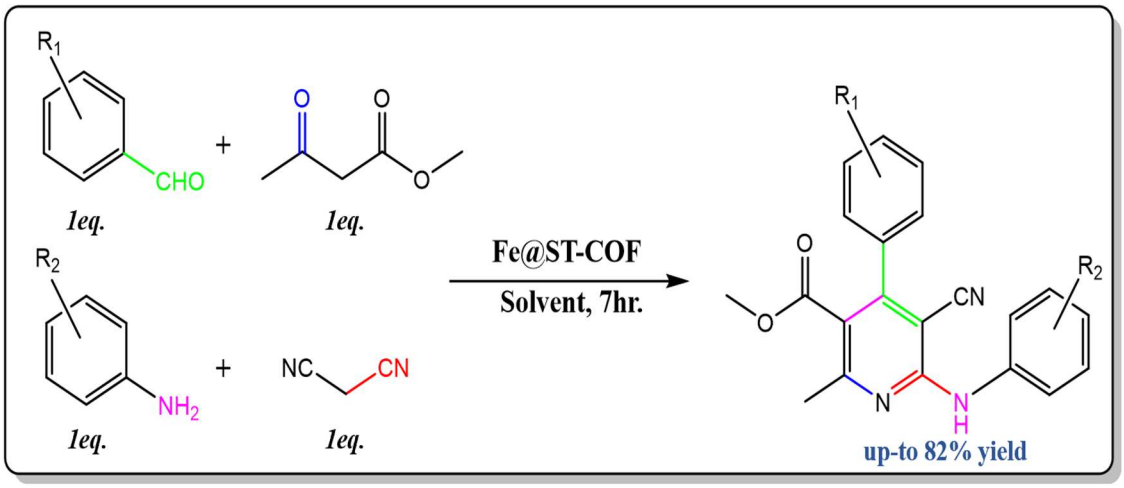

Scheme.5:- Fe(III)@ST-COF Catalyzed Four Component Addition/Cyclization Yielding Polysubstituted Pyridine.

3.3 Plausible Mechanism:

The proposed mechanism involves a Fe@ST-COF catalysed one-pot multicomponent reaction:

The reaction proceeds via a Fe@ST-COF-catalyzed one-pot multicomponent process. Initially, Fe@ST-COF activates the aldehyde to facilitate **Knoevenagel condensation** with malononitrile, forming an arylidene intermediate. It also activates methyl acetoacetate for a **Michael addition**, followed by **Schiff base** formation between the amine and carbonyl group. This leads to cyclization and subsequent tautomerization. Finally, Fe@ST-COF undergoes reduction to oxidize the intermediate, promoting aromatization and completion of the nicotinate scaffold. The catalyst plays a dual role by activating substrates and facilitating **oxidative aromatization**.

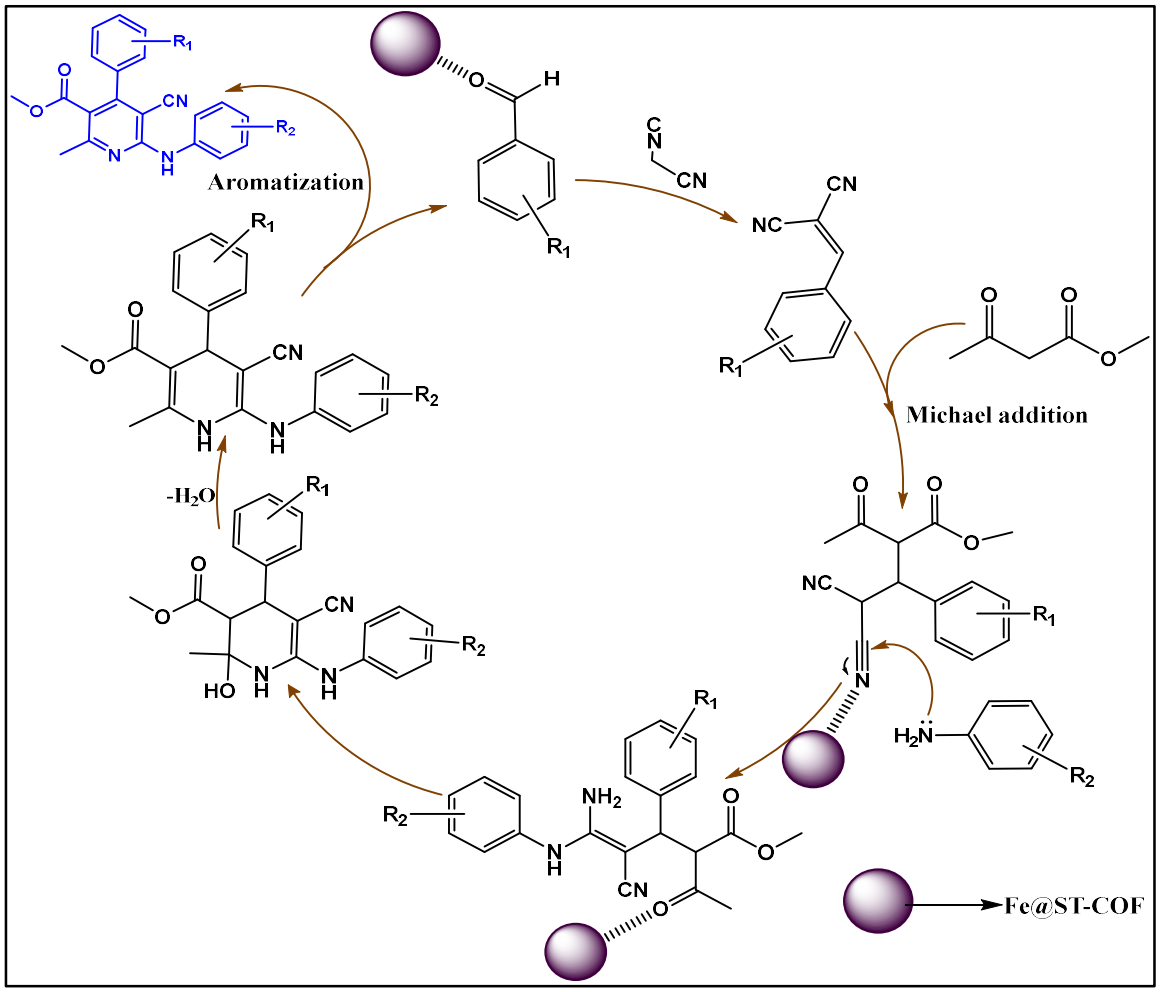

Fig.28:- Plausible reaction mechanism route.

3.4 Experimental Section:

3.4.1 Material Required:

To make the compound, we mixed several basic chemicals — aniline, p-nitro benzaldehyde, malononitrile, and methyl acetoacetate — along with a catalyst called Fe@ST-COF that speeds up the reaction. All the ingredients were used straight from the store without any extra cleaning. Everything was combined in a closed tube and gently heated. We used a simple method called TLC (Thin Layer Chromatography) to check how the reaction was going. Different liquids like alcohol and water were tested to find the best one for the reaction. After the reaction was done, we cleaned up the final product using a method that separates out the pure part (called column chromatography). We then confirmed the structure and quality of what we made using tools that look at how molecules behave (like IR and NMR machines) and also checked how easily it melts. All the detailed results are provided in the extra information section.

3.4.2 General procedure for synthesis of methyl 5-cyano-2-methyl-4-(4-nitrophenyl)-6-(phenylamino)nicotinate:

A solution was prepared by mixing aniline (1 mmol), p-nitrobenzaldehyde (1 mmol), malononitrile (1 mmol), methyl acetoacetate (1 mmol), and Fe@ST-COF catalyst (25 mg) in 6 mL of solvent i.e., ethanol . The reaction mixture was then heated under reflux conditions which is 70 °C in an oil bath. The progress of the reaction was monitored using thin-layer chromatography (TLC).After the reaction was complete, the mixture was cooled to room temperature and filtered to remove the Fe@ST-COF catalyst. The filtrate was then concentrated, and the crude product was purified by column chromatography using silica gel with ethyl acetate and n-hexane in a 7:3 ratio as the eluent. The purified product was obtained in 82% yield and characterized using NMR (recorded in DMSO-d_6 or $CDCl_3$). The melting point (208 °C) was also measured to confirm the product's identity and purity.

3.4.3 Observations on Table.1:

The catalytic efficiency of various systems was evaluated for the synthesis reaction. In the absence of a catalyst or when using $CuSO_4 \cdot 5H_2O$ alone, only trace yields were observed, highlighting the need for a more active catalyst. $FeCl_3$ showed moderate performance with a 65% yield, whereas Fe@ST-COF demonstrated superior catalytic activity, achieving up to 82% yield. Solvent screening revealed that ethanol was the most effective medium with Fe@ST-COF, consistently delivering high yields. Mixtures such as water/ethanol and methanol also provided reasonable yields of 62% and 70%, respectively, while non-polar or aprotic solvents like toluene, DMF, and acetonitrile were largely ineffective, resulting in only trace product formation. Catalyst loading studies indicated that increasing the amount of Fe@ST-COF significantly enhanced the yield: 15 mg gave a trace amount, 20 mg yielded 67%, and 25 mg resulted in the maximum yield of 82%. Reaction condition optimization further revealed that elevated temperatures (≥70°C) combined with an appropriate solvent notably improved the efficiency, and the reaction time could be reduced from 24 to 7 hours without compromising the yield under optimal conditions. Overall, the best outcome was achieved using 25 mg of Fe@ST-COF in ethanol at 70°C for 7 hours, demonstrating the critical influence of catalyst type, loading, and solvent choice on the reaction efficiency.

Table.1: Effect of Solvent , temperature, and amount of catalyst for catalyzing reaction:

S.N	Catalyst	Solvent	Temperature(°C)	Time(hr.)	Yield(%)
1	No Catalyst	Ethanol	70	24	trace
2	$CuSO_4.5H_2O$	Toluene	100	24	trace
3	$CuSO_4.5H_2O$	Ethanol	70	24	37
4	$FeCl_3$	Ethanol	70	24	65
5	Fe@ST-COF	DMF	100	12	trace
6	Fe@ST-COF	H_2O:ethanol	90	14	62
7	Fe@ST-COF	Toluene	100	12	trace
8	Fe@ST-COF	Acetonitrile	65	12	trace
9	Fe@ST-COF	Methanol	70	7	70
10	Fe@ST-COF(15mg)	Ethanol	70	24	trace
11	Fe@ST-COF(20mg)	Ethanol	70	7	67
12	**Fe@ST-COF(25mg)**	**Ethanol**	**70**	**7**	**82**

Reaction conditions: Fe@ST-COF, aniline (1 mmol), p-nitrobenzaldehyde (1 mmol), malononitrile (1 mmol), methyl acetoacetate (1mmol) and 6ml solvent, at reflux temperature.

Table 2: Synthesis of various derivatives of poly-substituted pyridine:

Entry	Product	Yield (%)	Time(hr.)	M.P(°C)
1	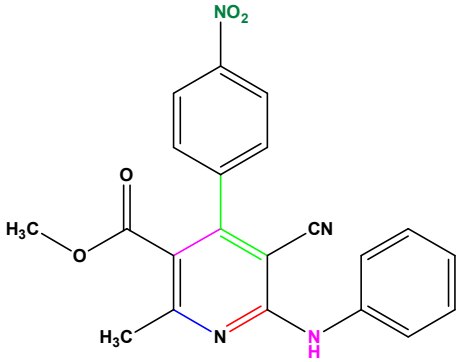	82	7	205-208
2	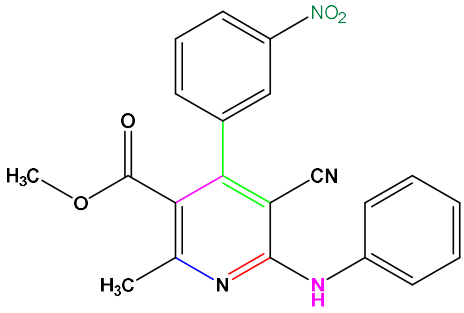	78	7	203-205
3	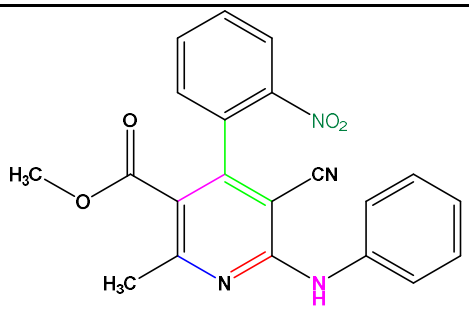	71	7	203-205
4	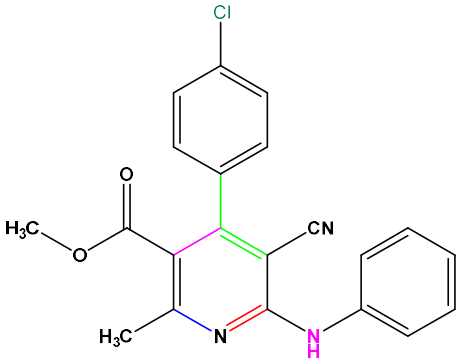	74	7	184-187

3.5 NMR Spectral Data: (2).NMR of methyl 5-cyano-2-methyl-4-(4-nitrophenyl)-6-(phenylamino)nicotinate

(a).^{1}H NMR (400 MHz, DMSO-d_6): δ 8.72 (s, 1H), 8.23 (d, J = 8.5 Hz, 2H), 7.48 (d, J = 8.5 Hz, 2H), 7.30 (d, J = 8.5 Hz, 2H), 6.87 (d, J = 8.5 Hz, 2H), 4.67 (s, 1H), 3.35 (s, 3H), 2.34 (s, 3H)

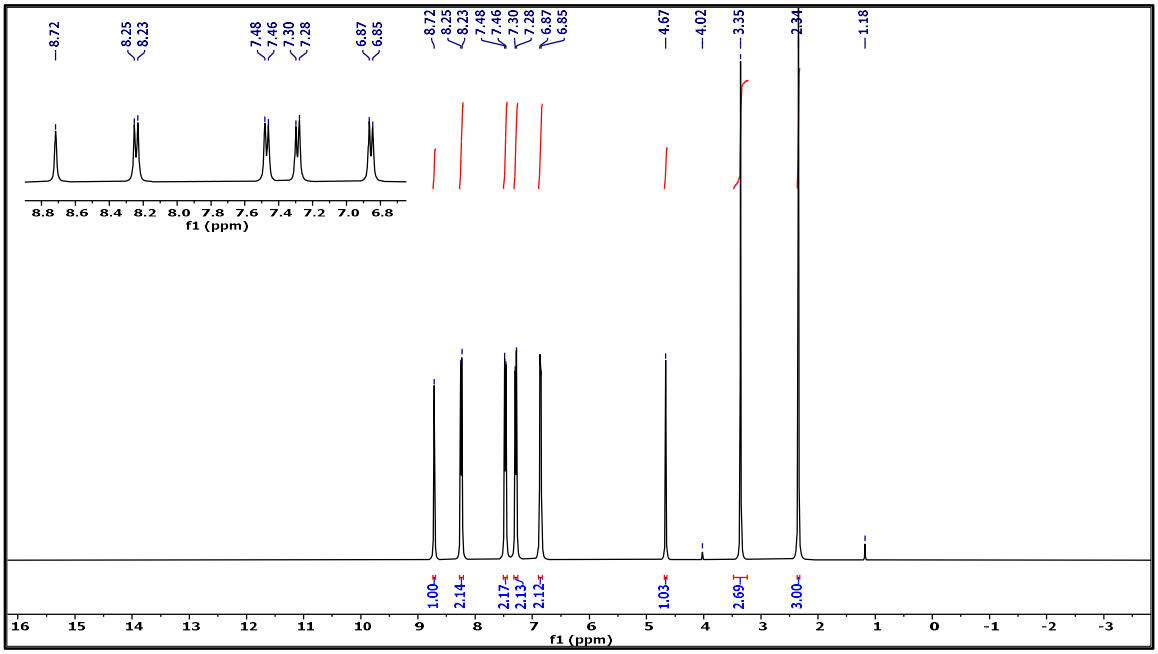

(b).^{13}C NMR(100 MHz, DMSO-d_6): δ 166.25, 164.90, 153.12, 148.45, 134.82, 132.75, 129.98, 127.62, 125.39, 118.17, 116.85, 113.47, 101.64, 51.23, 24.28.

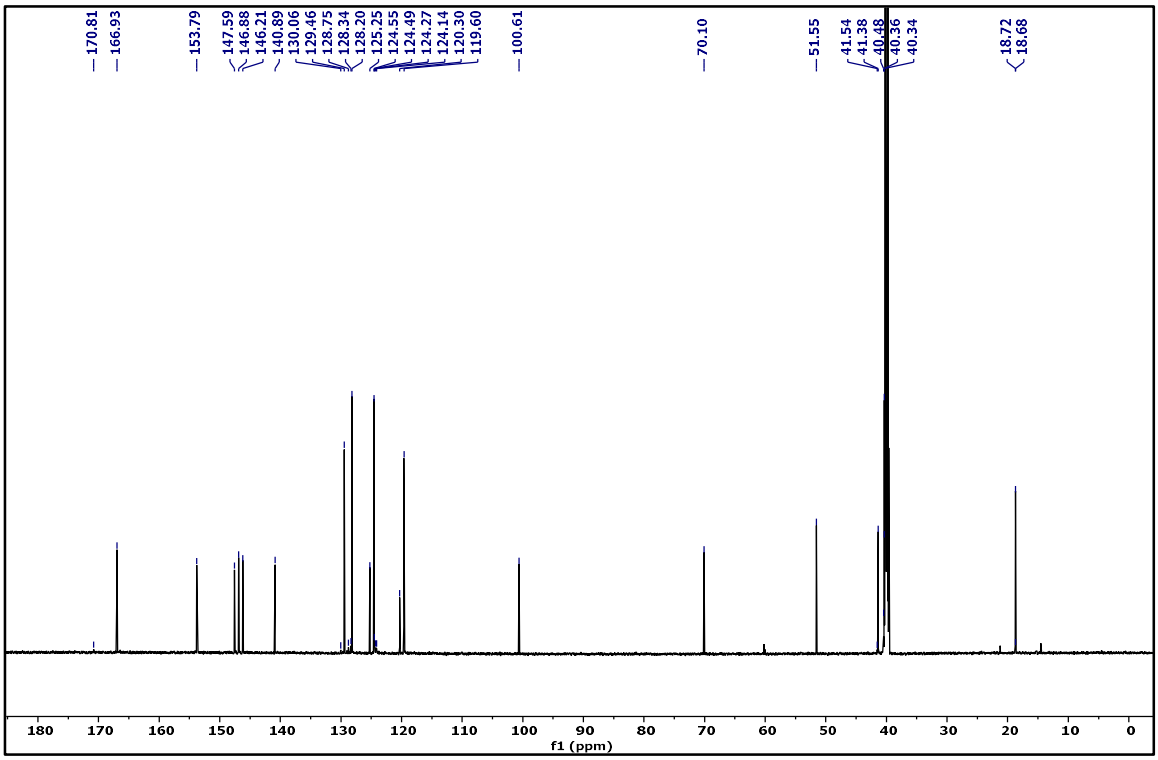

3.6 Conclusion:

In this study, a novel iron-incorporated covalent organic framework, Fe@ST-COF, was successfully synthesized through a multi-step approach beginning with the construction of a porphyrin-based COF (ST-COF). The framework was prepared via the condensation of meso-tetrakis(4-aminophenyl)porphyrin (TAPP) and 4,4'-(ethyne-1,2-diyl)dibenzaldehyde (SL-1) under solvothermal conditions using o-dichlorobenzene, n-butanol, and acetic acid as reaction media. The ST-COF thus formed was subsequently loaded with Fe^{3+} ions via simple coordination using $FeCl_3$ in methanol, resulting in the formation of Fe@ST-COF.

A range of advanced analytical techniques were employed to confirm the successful synthesis and modification of the COF. FT-IR spectroscopy showed the disappearance of the aldehyde C=O peak and the appearance of a strong C=N signal in ST-COF, along with Fe–N peaks in Fe@ST-COF. XRD analysis confirmed the crystalline nature of the ST-COF and the incorporation of Fe, as shown by broadened peaks and additional signals matching $FeCl_3$. TGA analysis demonstrated good thermal stability for both materials, with ST-COF showing slightly higher resistance to decomposition. BET surface area analysis showed a mesoporous structure in ST-COF with a surface area of 65.37 m^2/g, a pore volume of 0.0894 cc/g, and an average pore radius of 1.63 nm.

XPS analysis further confirmed the presence of iron in the +3-oxidation state through Fe $2p_{3/2}$ and $2p_{1/2}$ peaks at 711.2 eV and 724.4 eV, respectively. The full elemental survey detected only carbon, nitrogen, oxygen, and iron—confirming a clean synthesis without impurities. FESEM images revealed that both ST-COF and Fe@ST-COF have spherical morphology with Fe@ST-COF showing a rougher surface due to iron incorporation. EDS and elemental mapping supported these findings, showing 5.8 wt.% Fe in the loaded material, alongside appropriate C and N content.

Importantly, Fe@ST-COF was evaluated as a heterogeneous catalyst in a one-pot, four-component reaction involving aniline, p-nitrobenzaldehyde, malononitrile, and methyl acetoacetate. The catalyst showed excellent efficiency under mild conditions (ethanol, 70 °C, 7 h), giving a high yield of 82% of the target compound methyl 5-cyano-2-methyl-4-(4-nitrophenyl)-6-(phenylamino)nicotinate. The optimized conditions clearly

demonstrated that Fe@ST-COF outperforms other catalysts like $FeCl_3$ or $CuSO_4$, especially in green solvents such as ethanol.

This work highlights the remarkable potential of Fe@ST-COF as a sustainable, reusable, and effective catalyst for multicomponent reactions. Its large surface area, stable structure, and active metal sites make it highly suitable for practical applications in green organic synthesis, particularly for the synthesis of polysubstituted pyridine derivatives relevant to pharmaceuticals and materials science. The strategy demonstrated here contributes meaningfully to the development of metal-functionalized COFs for future catalytic technologies.

References

[1] "[1] J. Thote, H. B. Aiyappa, A. Deshpande, D. Díaz Díaz, S. Kurungot, and R. Banerjee, "A Covalent Organic Framework–Cadmium Sulfide Hybrid as a Prototype Photocatalyst for Visible-Light-Driven Hydrogen Production," Chemistry-A European Journal, vol. 20,".

[2] "[2] S. Y. Ding et al., "Construction of covalent organic framework for catalysis: Pd/COF-LZU1 in Suzuki-Miyaura coupling reaction," J Am Chem Soc, vol. 133, no. 49, 2011, doi: 10.1021/ja206846p.".

[3] "[3] P. Pachfule, S. Kandambeth, D. Díaz Díaz, and R. Banerjee, "Highly stable covalent organic framework-Au nanoparticles hybrids for enhanced activity for nitrophenol reduction," Chemical Communications, vol. 50, no. 24, 2014, doi: 10.1039/c3cc49176e.".

[4] "[4] P. Pachfule, M. K. Panda, S. Kandambeth, S. M. Shivaprasad, D. D. Díaz, and R. Banerjee, "Multifunctional and robust covalent organic framework-nanoparticle hybrids," J Mater Chem A Mater, vol. 2, no. 21, 2014, doi: 10.1039/c4ta00284a.".

[5] "[5] A. C. McKinlay et al., "BioMOFs: Metal-organic frameworks for biological and medical applications," Angewandte Chemie - International Edition, vol. 49, no. 36. 2010. doi: 10.1002/anie.201000048.".

[6] "[6] J. Jiang, J. Yu, and A. Corma, "Extra-large-pore zeolites: bridging the gap between micro and mesoporous structures," Angewandte Chemie - International Edition, vol. 49, no. 18. 2010. doi: 10.1002/anie.200904016.".

[7] "Y. Shi, Y. Wan, and D. Zhao, "Ordered mesoporous non-oxide materials," Chem Soc Rev, vol. 40, no. 7, 2011, doi: 10.1039/c0cs00186d.".

[8] "H. M. El-Kaderi et al., "Designed synthesis of 3D covalent organic frameworks,"".

[9] "[9] F. J. Uribe-Romo, J. R. Hunt, H. Furukawa, C. Klöck, M. O'Keeffe, and O. M. Yaghi, "A crystalline imine-linked 3-D porous covalent organic framework," J Am Chem Soc, vol. 131, no. 13, 2009, doi: 10.1021/ja8096256.".

[10] "[10] F. J. Uribe-Romo, C. J. Doonan, H. Furukawa, K. Oisaki, and O. M. Yaghi, "Crystalline covalent organic frameworks with hydrazone linkages," J Am Chem Soc, vol. 133, no. 30, 2011, doi: 10.1021/ja204728y.".

[11] "[11] T. E. Reich, S. Behera, K. T. Jackson, P. Jena, and H. M. El-Kaderi, "Highly selective CO 2/CH 4 gas uptake by a halogen-decorated borazine-linked polymer," J Mater".

[12] "[12] Y. Qin, X. Zhu, and R. Huang, "Covalent organic frameworks: linkage types, synthetic methods and bio-related applications," Biomaterials Science, vol. 11, no. 21. 2023. doi: 10.1039/d3bm01247f.".

[13] “[13] X. Wang, H. Liu, J. Zhang, and S. Chen, “Covalent organic frameworks (COFs): a promising CO2 capture candidate material,” Polymer Chemistry, vol. 14, no. 12. 2023. doi: 10.1039/d2py01350a.”.

[14] “[14] Y. Zhang et al., “New potential of boron-based COFs: the biocompatible COF-1 for reactive oxygen generation and antimicrobial applications,” J Mater Chem B, vol. 10, no. 17, 2022, doi: 10.1039/d1tb02808a.”.

[15] “[15] H. Chen et al., “Triazine-Based Covalent Organic Framework for Photocatalytic Water Oxidation: The Role of Bipyridine Ligand and Cobalt Coordination,” Journal of”.

[16] “[18] M. Afshari, M. Dinari, H. Farrokhpour, and F. Zamora, “Imine-Linked Covalent Organic Framework with a Naphthalene Moiety as a Sensitive Phosphate Ion Sensing,” ACS Appl Mater Interfaces, vol. 14, no. 19, 2022, doi: 10.1021/acsami.1c24555.”.

[17] “[17] “Erratum: Generation of covalent organic framework-derived porous N-doped carbon nanosheets for highly efficient electrocatalytic hydrogen evolution (Energy Adv. (2023) DOI: 10.1039/d3ya00325f),” Energy Advances, vol. 2, no. 11. 2023. doi: 10.1039/d3”.

[18] “X. Li et al., “Expeditious synthesis of covalent organic frameworks: A review,””.

[19] “[16] J. Maschita, T. Banerjee, and B. V. Lotsch, “Direct and Linker-Exchange Alcohol-Assisted Hydrothermal Synthesis of Imide-Linked Covalent Organic Frameworks,” Chemistry of Materials, vol. 34, no. 5, 2022, doi: 10.1021/acs.chemmater.1c04051.”.

[20] “[15] H. Chen et al., “Triazine-Based Covalent Organic Framework for Photocatalytic Water Oxidation: The Role of Bipyridine Ligand and Cobalt Coordination,” Journal of”.

[21] “[19] X. Li et al., “Solvothermal Synthesis of Uniform Covalent Organic Framework Microspheres Enabling High-Loading Palladium for Oxygen Reduction Reaction,” Macromolecules, vol. 56, no. 12, 2023, doi: 10.1021/acs.macromol.3c00393.”.

[22] “[17] “Erratum: Generation of covalent organic framework-derived porous N-doped carbon nanosheets for highly efficient electrocatalytic hydrogen evolution (Energy Adv. (2023) DOI: 10.1039/d3ya00325f),” Energy Advances, vol. 2, no. 11. 2023. doi: 10.1039/d3”.

[23] “[20] Q. Guan, G. B. Wang, L. Le Zhou, W. Y. Li, and Y. Bin Dong, “Nanoscale covalent organic frameworks as theranostic platforms for oncotherapy: Synthesis, functionalization, and applications,” Nanoscale Advances, vol. 2, no. 9. 2020. doi: 10.1039/d0na00”.

[24] “[23] D. D. Medina et al., “Room temperature synthesis of covalent-organic framework films through vapor-assisted conversion,” J Am Chem Soc, vol. 137, no. 3, 2015, doi: 10.1021/ja510895m.”.

[25] “[24] R. K. Sharma et al., “Recent development of covalent organic frameworks (COFs): Synthesis and catalytic (organic-electro-photo) applications,” Materials Horizons, vol. 7, no. 2. 2020. doi: 10.1039/c9mh00856j.”.

[26] “[26] J. N. Chang et al., “Oxidation-Reduction Molecular Junction Covalent Organic Frameworks for Full Reaction Photosynthesis of H2O2,” Angewandte Chemie - International Edition, vol. 62, no. 9, 2023, doi: 10.1002/anie.202218868.”.

[27] “[27] J. Alemán and R. Mas-Ballesté, “Photocatalytic Oxidation Reactions Mediated by Covalent Organic Frameworks and Related Extended Organic Materials,” Front Chem, vol. 9, 2021, doi: 10.3389/fchem.2021.708312.”.

[28] “[28] E. Rozhko, A. Bavykina, D. Osadchii, M. Makkee, and J. Gascon, “Covalent organic frameworks as supports for a molecular Ni based ethylene oligomerization catalyst for the synthesis of long chain olefins,” J Catal, vol. 345, 2017, doi: 10.1016/j.jcat.”.

[29] “https://pubs.acs.org/doi/10.1021/acsami.3c15766”.

[30] “[29] X. Yang et al., “Charging modulation of the pyridine nitrogen of covalent organic frameworks for promoting oxygen reduction reaction,” Nat Commun, vol. 15, no. 1, 2024, doi: 10.1038/s41467-024-46291-y.”.

[31] “[30] M. Ni, M. K. H. Leung, D. Y. C. Leung, and K. Sumathy, “A review and recent developments in photocatalytic water-splitting using TiO2 for hydrogen production,” Renewable and Sustainable Energy Reviews, vol. 11, no. 3. 2007. doi: 10.1016/j.rser.2005.0”.

[32] “[35] P. Ghosh and P. Banerjee, “Drug delivery using biocompatible covalent organic frameworks (COFs) towards a therapeutic approach,” Chemical Communications, vol. 59, no. 84. 2023. doi: 10.1039/d3cc01829f.”.

[33] “[33] C. Qian et al., “Conductive Covalent Organic Frameworks Meet Micro-Electrical Energy Storage: Mechanism, Synthesis and Applications—A Review,” Crystals, vol. 12, no. 10. 2022. doi: 10.3390/cryst12101405.”.

[34] “[31] L. Jin, S. Lv, Y. Miao, D. Liu, and F. Song, “Recent Development of Porous Porphyrin-based Nanomaterials for Photocatalysis,” ChemCatChem, vol. 13, no. 1. 2021. doi: 10.1002/cctc.202001179.”.

[35] “[37] M. Li et al., “A cage-based covalent organic framework for drug delivery,” New Journal of Chemistry, vol. 45, no. 6, 2021, doi: 10.1039/d0nj04941g.”.

[36] “[38] M. X. Wu and Y. W. Yang, “Applications of covalent organic frameworks (COFs): From gas storage and separation to drug delivery,” Chinese Chemical Letters, vol. 28, no. 6. 2017. doi: 10.1016/j.cclet.2017.03.026.”.

[37] “[39] I. J. Gomez, B. Arnaiz, M. Cacioppo, F. Arcudi, and M. Prato, “Nitrogen-doped Carbon Nanodots for bioimaging and delivery of paclitaxel,” J Mater Chem B, vol. 6, no. 35, 2018, doi: 10.1039/x0xx00000x.”.

[38] K. Zhao, “Porphyrin-based COF nanosheet arrays with donor-acceptor structure for solar-driven water purification.,” no. https://doi.org/10.1016/j.desal.2024.117956.

[39] “FeCl 3 Catalyzed Four-Component Nucleophilic Addition/Intermolecular Cyclization Yielding Polysubstituted PyridineDerivativesXinwei He, Yongjia Shang,* Zhiyu Yu, Mei Fang, Yao Zhou, Guang Han, and Fuli Wu”.”.

[40] “Ghosh, S.; Das, S.; Das, S.; Paul, S.; Maiti, D.$FeCl_3$-Catalyzed Synthesis of Symmetrical Pyridines from Ketoxime Acetates and DMFDMA.DOI: 10.1080/10406638.2023.2254895”.

[41] “Mari, G.; De Crescentini, L.; Favi, G.; Mantellini, F.; Santeusanio, S.Challenge N- versus O-Six-Membered Annulation: $FeCl_3$-Catalyzed Synthesis of Heterocyclic N,O-Aminals.DOI: 10.3762/bjoc.20.123”.

[42] “Zhang, Y.; Li, X.; Wang, H.; Liu, Y.; Zhao, Y.$FeCl_3$-Catalyzed One-Pot Synthesis of Polysubstituted Pyridines via a Three-Component Reaction.DOI: 10.1016/j.tetlet.2015.09.055”.

[43] “Li, H.; Wang, Y.; Zhang, Y.; Liu, X.; Chen, J.$FeCl_3$-Catalyzed Cascade Reaction: An Efficient Approach to Polysubstituted Pyridines.DOI: 10.1002/jhet.2391”.

[44] “Kumar, A.; Singh, R.; Sharma, P.; Gupta, R.$FeCl_3$-Catalyzed Synthesis of Polysubstituted Pyridines via a One-Pot Multicomponent Reaction.DOI: 10.1007/s00706-016-1881-2”.

[45] “Sadawarte, G., Jagatap, S., Patil, M., Jagrut, V., & Rajput, J. D. (2021). Synthesis of substituted pyridine-based sulphonamides as an antidiabetic agent. European Journal of Chemistry, 12(3), 279–283. DOI: 10.5155/eurjchem.12.3.279-283.2118”.

[46] “El-Naggar, M. A., El-Agrody, A. M., Badr, A. M., & Abdel-Gawad, S. M. (2021). Synthesis of new substituted pyridine derivatives as potent anti-liver cancer agents through apoptosis induction: In vitro, in vivo, and in silico integrated approaches. Bioorga”.

[47] “Khan, A. M., Khan, M., Shahid, M., & Kumar, S. (2022). Medicinal importance and chemosensing applications of pyridine derivatives: A review. Critical Reviews in Analytical Chemistry. DOI: 10.1080/10408347.2022.2089839”.

[48] “Patel, P., Patel, H., Parmar, A., & Patel, M. (2023). Recent advances in pyridine scaffold: Focus on chemistry, synthesis, and antibacterial activities. Molecules, 28(3), 1026. DOI: 10.3390/molecules28031026”.

[49] “Zhu, C., Yang, B., Zhao, Y., Fu, C., Tao, L., & Wei, Y. (2013). A new insight into the Biginelli reaction: the dawn of multicomponent click chemistry? Polymer Chemistry, 4(21), 5395–5400. DOI: 10.1039/C3PY00553D”.

[50] “Zhu, Y.-L., Huang, S.-L., & Pan, Y.-J. (2005). Highly chemoselective multicomponent Biginelli-type condensations of cycloalkanones, urea or thiourea and aldehydes. European Journal of Organic Chemistry, 2005(11), 2354–2367. DOI: 10.1002/ejoc.200400845”.

[51] “De Souza, R. O. M. A., da Penha, E. T., Milagre, H. M. S., Garden, S. J., Esteves, P. M., Eberlin, M. N., & Antunes, O. A. C. (2009). The three-component Biginelli reaction: a

combined experimental and theoretical mechanistic investigation. Chemistry – A". DOI: 10.1002/chem.200900470